SUNDSTRAND

SUNDSTRAND TURBO

S/TD NO. 1735

STUDY OF TURBINE AND TURBOPUMP DESIGN PARAMETERS

FINAL REPORT - VOLUME II
A STUDY OF HIGH PRESSURE DRAG TURBINES USING COMPRESSIBLE FLUIDS

Robert Spies

Contract No. NONR-2292(00)
Task No. NR 094-343

For the period 1 February 1958 through
30 January 1960

Department of the Navy
Office of Naval Research

SUNDSTRAND TURBO
DIVISION OF SUNDSTRAND CORPORATION

FOREWORD

This document was prepared by the Turbine Research Section of the Sundstrand Turbo Division of the Sundstrand Corporation and is submitted in fulfillment of U. S. Navy Contract Nonr 2292(00) No. NR 094 343. It is the second of four parts comprising the final report. The work reported in this volume was performed between 1 February 1958 and 30 January 1960.

The original turbine design and analysis were the work of Mr. W. Nerenstein. The author acted as Project Engineer during the final phases. Mr. M. B. Dubey supervised the program as Head of the Turbine Research Section. Messrs. H. Gavenman, F. Beach, and H. Goodknight assisted with hardware procurement and testing, and Mrs. R. E. Deere with the data evaluation. Dr. O. E. Balje, Principal Investigator, reviewed the report and consulted on technical problems.

Approved by:

O. E. Balje
Principal Investigator

E. B. Zwick
Associate Chief Engineer

W. E. Wayman
Chief Engineer

TABLE OF CONTENTS

LIST OF ILLUSTRATIONS

LIST OF ILLUSTRATIONS (Continued)

I. OBJECTIVE

The objective of this program is the study of a large-pressure-ratio drag turbine using a compressible fluid, and the verification of the simplified drag-turbine theory presented in Reference 1.

II. SUMMARY

The simplified drag-turbine theory presented by Balje in Reference 1 and discussed in Reference 2 has been extended to cover the case of a compressible gas in a turbine of arbitrary area distribution. Conclusions regarding superior performance when an expanding channel is used have been verified and areas of future investigations indicated. The attainable efficiency of a large pressure-ratio drag-turbine is high with values of 44 percent anticipated in future designs.

III. TECHNICAL DISCUSSION

A. Theory

1. The simplified drag-turbine theory utilizes a one-dimensional approximation to explain performance. Thus, while it is realized that the flow through the turbine is extremely complex, the notion of a unidirectional flow which pulls, or drags, the rotor as it passes by it, is utilized. The work output is computed by using an average friction coefficient

for the rotor and the equivalent one-dimensional velocity past the rotor. It is noted that (neglecting the secondary effects of curvature) the drag is

$$D = \int \tau_r \, da_r \qquad (1)$$

with the integral taken around the rotor. The shear stress is defined as

$$\tau_r = \frac{\gamma}{2g} (c-u)^2 \lambda_r \qquad (2)$$

where

γ = density (#/ft^3)

c = throughflow velocity (fps)

u = rotor velocity (fps)

λ_r = rotor friction factor

The work output is

$$W = \int \frac{D u}{\dot{w}}$$

$$= \int \frac{u}{c} \lambda_r \frac{(c-u)^2}{2g} \frac{da_r}{A} \qquad (3)$$

where

da_r = differential rotor area (ft^2)

A = throughflow area (ft^2)

and the continuity equation

$$\dot{w} = \gamma A c \tag{4}$$

has been substituted.

2. In general, the flow through the turbine can be analyzed by the use of the momentum, the energy, and the state equations.

Momentum equation:

$$\frac{dp}{\gamma} + \frac{c\,dc}{g} = -\left[\lambda_s \frac{c^2}{2g} \frac{da_s}{A} + \lambda_r \frac{(c-u)^2}{2g} \frac{da_r}{A}\right] \tag{5}$$

Energy equation:

$$c_p dt + \frac{c\,dc}{g} + dW = dQ \tag{6}$$

Equation of state:

$$p = \gamma R t \tag{7}$$

where the subscript $(\quad)_s$ refers to the stator.

3. The input head is (following the usage in previous papers on drag turbines)

$$H_{IN} = -\int \frac{dp}{\gamma} - \int \frac{c\,dc}{g} \tag{8}$$
$$= \int \lambda_s \frac{c^2}{2g} \frac{da_s}{A} + \int \lambda_r \frac{(c-u)^2}{2g} \frac{da_r}{A}$$

and the hydraulic efficiency is

$$\eta_H = \frac{W}{H_{IN}}$$

$$= \frac{\int \frac{u}{c} \lambda_r \frac{(c-u)^2}{2g} \frac{da_r}{A}}{\int \lambda_s \frac{c^2}{2g} \frac{da_s}{A} + \int \lambda_r \frac{(c-u)^2}{2g} \frac{da_r}{A}} \qquad (9)$$

Substituting

$$x = \frac{u}{c}$$

$$\eta_H = \frac{\int x \lambda_r \frac{(1-x)^2}{x^2} \frac{da_r}{A}}{\int \lambda_s \frac{1}{x^2} \frac{da_s}{A} + \int \lambda_r \frac{(1-x)^2}{x^2} \frac{da_r}{A}} \qquad (10)$$

4. For the special case of a turbine using an incompressible fluid and having a constant throughflow area, A, the continuity equation shows that c, and therefore x, is a constant. Hence, if the equivalent friction factor is used,

$$H_{IN} = \lambda_s \frac{c^2}{2g} \frac{a_s}{A} + \lambda_r \frac{(c-u)^2}{2g} \frac{a_r}{A}$$

$$= \frac{\tau_s a_s + \tau_r a_r}{\gamma A} \qquad (11)$$

and

$$\eta_H = \frac{x \lambda_r (1-x)^2 \frac{a_r}{A}}{\lambda_s \frac{a_s}{A} + \lambda_r (1-x)^2 \frac{a_r}{A}}$$

$$= \frac{x}{\frac{\delta}{(1-x)^2} + 1} \qquad (12)$$

where

$$\delta = \frac{\lambda_s a_s}{\lambda_r a_r}$$

Equations (11) and (12) are given in Reference 1, 2 and 3. As pointed out in these reports, the efficiency is a maximum for a particular value of the speed ratio x, and, if the turbine is designed for this velocity ratio, the highest efficiency of the turbine will be reached.

5. When a compressible fluid is used, the efficiency equation is not integrated as readily. However, some special cases can be discussed. For example, in the case of a constant throughflow-area channel, the hydraulic efficiency is

$$\eta_H = \frac{\int x \lambda_r \frac{(1-x)^2}{x^2} da_r}{\int \lambda_s \frac{1}{x^2} da_s + \int \lambda_r \frac{(1-x)^2}{x^2} da_r} \qquad (13)$$

With the throughflow area remaining constant, it is probable that both the rotor-surface area and the stator-surface area will increase linearly with the rotor angle, or

$$da_r = k_r \, d\theta$$
$$da_s = k_s \, d\theta \qquad (14)$$

In that case

$$\eta_H = \frac{k_r \int \chi \lambda_r \frac{(1-\chi)^2}{\chi^2} d\theta}{k_s \int \lambda_s \frac{1}{\chi^2} d\theta + k_r \int \lambda_r \frac{(1-\chi)^2}{\chi^2} d\theta} \qquad (15)$$

and it is necessary to know how x varies along the channel. The efficiency is computed for an assumed variation of x in Appendix B. The hydraulic efficiency will vary as the velocity ratio changes and the over-all efficiency of the turbine will be less than that of its most efficient segment. In the case of the incompressible fluid it was possible to design for the optimum velocity and efficiency at all points in the turbine, but in the constant-area compressible-flow turbine this is not possible.

6. It is also evident that it should be possible to choose the throughflow area distribution in such a way that the optimum value of efficiency is maintained at all points in the passage when operating at the design pressure ratio. This will mean that the velocity ratio will be nearly constant.

If the velocity ratio is constant Equation (10) becomes

$$\eta_H = \frac{\chi}{\frac{\lambda_s}{\lambda_r} \frac{1}{(1-\chi)^2} \frac{\int da_s/A}{\int da_r/A} + 1} \qquad (16)$$

and the efficiency is constant around the channel only if

$$\frac{\int \frac{da_s}{A}}{\int \frac{da_r}{A}} = I = \text{constant} \qquad (17)$$

for every interval $(\Theta_2 - \Theta_1)$. This may or may not be the case for practical design geometries.

7. It is desirable to keep the value of the integral ratio (Equation 17) as low as possible so that the efficiency will be high. Let

$$\frac{da_s}{d\Theta} = f_s(\Theta) \qquad (18)$$

$$\frac{da_r}{d\Theta} = f_r(\Theta)$$

$$A = A(\Theta)$$

Then

$$\frac{da_s}{A} = f_s \frac{d\Theta}{A} \qquad (19)$$

$$\frac{da_r}{A} = f_r \frac{d\Theta}{A}$$

and

$$I = \frac{\int f_s \frac{d\Theta}{A}}{\int f_r \frac{d\Theta}{A}}$$

Differentiation of the integral ratio yields the condition for the minimum value, or

$$\frac{f_s \frac{d\theta}{A}}{\int f_s \frac{d\theta}{A}} = \frac{f_r \frac{d\theta}{A}}{\int f_r \frac{d\theta}{A}} \tag{20}$$

Equation (20) indicates

$$f_s \frac{d\theta}{A} = k f_r \frac{d\theta}{A} \tag{21}$$

where k is a constant. The simplest solution is

$$f_s = k f_r$$

$$\frac{da_s}{d\theta} = k \frac{da_r}{d\theta} \tag{22}$$

The integral ratio is then

$$I = \frac{\int k f_r \frac{d\theta}{A}}{\int f_r \frac{d\theta}{A}} = k \tag{23}$$

so that best results are achieved when I is equal to k. The value of k is, of course, dictated by the amount the throughflow perimeter must increase to accomodate the constant-velocity condition. In most drag-turbines the

rotor-surface area will increase linearly, or

$$da_r = k_r \, d\theta$$

where (see Figure (1))

$$k_r = \frac{D-e}{2}(2e+2H')$$

$$= (D-e)(e+H') \qquad (24)$$

From Equation (22)

$$da_s = k \, da_r$$

$$= k \, k_r \, d\theta$$

so that

$$k_s = k \, k_r$$

$$= \left(\frac{D-e+f}{2}\right)(4H+2H'+2e+f) \qquad (25)$$

and

$$k = \frac{k_s}{k_r}$$

$$= \frac{(D-e+f)(2H+H'+e+f/2)}{(D-e)(e+H')} \qquad (26)$$

In these relations D, e, and H are constant. The other variables must be chosen to yield the proper throughflow area distribution

$$A = A(\theta)$$

where

$$A = 2Hb + 2H'f \tag{27}$$

8. The simplified drag-turbine theory presented here has assumed that it is possible to define an equivalent value of the friction coefficients (λ_r and λ_s) such that they may be assumed to be constant over the perimeter. It has, of course, been shown before, in Reference 2, that the rotor-friction coefficient is affected by the values of certain geometrical ratios, i.e.,

$$m = H'/H$$
$$\mu = D/H$$
$$Y = f/H$$
$$\varepsilon = D/d$$

and it is logical to suppose that, as the channel deverges, λ_r will vary. If the variation is not too great, an average value may be used. In the case under study here the parameters varied over the following ranges:

$$0.37 < m < 1.00$$
$$6.20 < \mu < 9.50$$
$$0.12 < Y < 0.44$$
$$\varepsilon = 1.20$$

From data available in Reference 4, it can be concluded that λ_r reaches a maximum value when $m > 0.3$ for blade angles of 25°, 35° and 45° when flat-topped blades are utilized. When the blades are rounded at the top (as was the case in the turbine tested) λ_r is much higher and values in excess of 0.25 are reached when $m > 0.3$. No optimum value is obtained in Reference 4. This reference also shows that, for 35° rounded blades, $\lambda_r = 0.3$ when, $8 < \mu < 20$, and 45° rounded blades $\lambda_r = 0.45$ for this range. The curves are fairly flat and are not expected to drop sharply as μ approaches 6.0. Unfortunately, the value of the tip-clearance ratio, γ, is zero in all these tests. However, Figure VI, 10 of Reference 1 shows that λ_r is fairly insensitive to changes in γ and values on the order of 0.4 to 0.45 are to be expected for $\mu \sim 10$.

9. It can be seen that the value of λ_r which is to be chosen in any design must depend on the values of the geometric parameters mentioned. If an application allows a choice where λ_r does not vary greatly over the periphery of the

pump, an average value may be used. If greater accuracy is desired, or if λ_r varies too greatly, it will be necessary to keep it under the integral sign in Equation (15) and to account for the variation.

B. Experimental Investigation

1. To verify the simplified drag-turbine theory proposed in Reference 1, a turbine was built and tested. As discussed in the previous section certain ratios relating to housing geometry have been found to give good performance. It may, therefore, be impossible to maintain the stator-surface-area distribution such that

$$\frac{da_s}{d\theta} = k_s$$

while keeping the correct throughflow area. Certain design compromises must therefore be made. Furthermore, machining practice may dictate certain other compromises so that the test turbine may not be able to attain the efficiency of the true constant-velocity turbine.

2. Because of these considerations, the test turbine was designed as shown in Figure 2. The resulting area distributions

are as shown in Figures 3 and 4. The calculated velocity distribution for a stall-torque test is shown in Figure 5. The original design objective had been a turbine-pressure ratio of 10:1 and constant throughflow velocity which corresponds to an area ratio of about 8:1. Unfortunately, no provision was made for the exhaust line in the design calculations so that the "correct" discharge area appears at the end of the channel (angular position = 350 degrees) and not at the start of the exit section (angular position = 300 degrees). The real area ratio is, therefore, less than anticipated. However, tests made during this program showed that the equivalent rotor friction coefficient, was independent of pressure ratio for this geometry so that test data reported at pressure ratios of 10:1 are valid. The larger pressure ratios are chosen because of the greater accuracy inherent in the larger readings.

3. The questions which must be answered are:

a. Is it possible to predict the output torque for a given drag turbine knowing only the inlet conditions and the pressure ratio?

b. Is a drag turbine using a compressible fluid and incorporating an expanding channel more efficient than the constant-area turbine?

If the answer to (a) is affirmative, then the simplified drag-turbine theory is valid and if (b) is true, then a new design criterion can be established.

4. The area distribution which was chosen for the turbine was based on a desire to achieve the maximum efficiency using all information available at that time. It was found that a constant-velocity channel would result in a geometric configuration where the friction coefficient would be low over part of the periphery. For this reason, the channel shape is neither constant area, nor is it such that constant velocity is maintained. However, since the area distribution is known, the flow equations can be solved and the pressure and velocity distribution found. It is necessary to use a step-wise integration process to do this, as shown in Appendix A. A value for the stator-friction factor, λ_s, equal to 0.007 was used. This is fairly typical for smooth walls. The result, which is a function of the friction factor, is shown in

Figures 5 through 8 for a stall-torque and a running test. It is seen that there exists a value of the rotor-friction factor which results in the correct back pressure (atmospheric) for the turbine*. The corresponding velocity curve can be used to compute the torque. For the stall-torque test, the computed value of 14.6 in.-lb. compares with a measured value of 15 in.-lb, while for the running test the values are 11.0 in.-lb computed and 11.4 in.-lb measured. The agreement is typical and very good. It is also interesting to observe the manner in which the measured pressure distribution compares with the predicted value. This is shown in Figures 9 and 10. Again the agreement is very good. It can be concluded, therefore, that the use of an equivalent friction coefficient yields the correct pressure distribution and the correct value for the torque produced.

---

* From the figures it might appear that very small changes in Δ will change the pressure distribution drastically. This is not necessarily the case. The velocity rises sharply just before the end of the channel and it becomes necessary to take smaller increments in the stepwise integration process. There is a limit to the practicality of this.

5. Since the scope of the program allowed for the test of only one turbine type, it was not possible to make a direct comparison between the constant-velocity drag turbine and the one incorporating a constant throughflow area. However, the performance of these units is somewhat predictable and some comparisons can be made. In the case of the constant-velocity turbine, it has been shown that the hydraulic efficiency is

$$\eta_H = \frac{X}{\frac{\delta_{eq}}{(1-x)^2} + 1} \tag{29}$$

where

$$\delta_{eq} = \frac{\lambda_s}{\lambda_r} \frac{\int da_s/A}{\int da_r/A}$$

It is usual to define the adiabatic efficiency as

$$\eta_{ad} = \frac{\int dW}{\int dH_{ad}} \tag{30}$$

where

$$\begin{aligned} dH_{ad} &= c_p t_1 \left[1 - \left(\frac{p+dp}{p}\right)^{\frac{k-1}{k}}\right] \\ &\doteq c_p t_1 \left[1 - \left(1 + \frac{k-1}{k}\frac{dp}{p}\right)\right] \\ &\doteq -\frac{dp}{\gamma} \end{aligned} \tag{31}$$

Since the input head was defined as

$$dH_{IN} = -\frac{dp}{\gamma} - \frac{c\,dc}{g}$$

the two are the same when dc = 0. For this reason, the hydraulic efficiency equals the adiabatic efficiency in this case.

6. The test results reported before indicate values for λ_r, λ_s, k_r and k_s. It appears that

$$\delta_a = 0.06$$

which is a reasonable value. For it, $(\eta_H)_{max}$ = 44 percent when the velocity is constant. It can, therefore, be stated that the constant-velocity drag turbine would reach a maximum efficiency of 44 percent. If the turbine is designed to keep the throughflow area constant, then the use of the equation in Appendix B shows that the maximum hydraulic efficiency is a function of the density ratio, γ_o/γ_f. The adiabatic efficiency is

$$\eta_{ad} = \frac{\int dW}{\int dH_{ad}}$$

$$= \frac{\int dW}{\int dH_{IN} + \int \frac{c\,dc}{g}}$$

$$= \frac{1}{\eta_H + \int \frac{c\,dc}{g} / \int dW}$$

This shows that when the velocity is not constant a slight difference in efficiency will result. It should be noted that wheel disc friction has been neglected.

7. The efficiency of the turbine is shown in Figures 11, 12, and 13. For comparison, the maximum attainable efficiency for constant velocity and constant area is also shown. It can be seen that the tests show a maximum efficiency in between those of the constant-velocity and constant-area case. This is to be expected since, as pointed out before, the tests turbine achieved neither goal. It is obvious that expanding the throughflow channel had the desired result of increasing the efficiency and it is to be expected that a more sophisticated design resulting in a more

uniform throughflow velocity will result in even higher efficiency, providing it is still possible to assume that λ_r remains constant.

8. The turbine was tested using three inlet configurations. The original inlet injected the fluid from above. Subsequent to this, the fluid was injected from the side. The area of admission was considerably smaller for this case. To make a direct comparison, the top inlet was closed down until the area was nearly equal to the side-inlet area. Figures 14 and 15 shows the inlet geometry. It was observed that the smaller openings restricted the flow sufficiently to cause a large pressure loss at the inlet; that this loss was greater for the top inlet; that the pressure distribution for the two top inlets was the same; and that the side inlet resulted in a slightly different distribution than the top inlet. These results are shown in Figure 16.

9. It is interesting to note that the value of the measured rotor-friction factor is large enough to yield values of $\delta_{eq}=0.06$. This value is lower than previously anticipated in References 1 and 2, and would yield very high efficiency in a constant-

velocity turbine. The difference is attributable to the rotor-blade shape which is shown in Figure 17 and which utilizes a curved rear face for the blades. This helps to "trap" the fluid and induces a special vortex flow. It is based on data found in Reference 4 where friction factors as high as 0.5 are reported. This result is significant enough to warrant further investigation.

C. Test Equipment

1. Figure 18 is an over-all view of the control room of the Turbine Test Laboratory. Figure 19 shows the console used in monitoring the test and Figure 20 shows the turbine mounted on its stand.

2. The turbine is composed of a vaned rotor turning in a housing. Figure 21 is a picture of the components. The geometry of the rotor blades is shown in Figure 17.

D. Instrumentation

1. A diagram showing the location of all gages is shown in Figure 22. The make and accuracy of each gage is listed in Table I. Consistency of the test results in shown in Figure 23.

2. Torque measurements were made using a Wiancko Engineering Company force ring in conjunction with an electric generator dynamometer and carrier oscillator. The oscillator serves as a power source to the deflection-measuring force ring. The deflection is translated into in.-lbs. readings on a Simpson Meter by a demodulation unit. The force ring has a range of ±20 lbs with an accuracy of 0.5 percent and is placed at a radius of 10 in. giving a range up to ±200 in.-lb. The Simpson meter has a range of 0-100 in.-lb with an accuracy of 1 percent of full scale.

3. The wheel speed was measured by a magnetic pickup using two lobes on a coupling. A Hewlett Packard Electronic Counter with a range of 0 - 99,999 cps was used. Its accuracy is 0.1 percent.

IV. CONCLUSION

The theory for drag-turbine operation presented by Balje in Reference 1 has been verified. By a modification of the equations to include the case of the compressible fluid in any channel it has been possible to predict the performance of the turbine. Furthermore, it has been shown that the test turbine,

which had an expanding channel (although it did not produce a constant velocity distribution) was more efficient than the equivalent constant-area turbine. It was less efficient than the constant-velocity turbine. Operation of the turbine has shown that a value for

$$\delta_{eq} = 0.06$$

is reasonable. This is lower than previously suspected and is responsible for the high efficiency level predicted for the constant-velocity turbine (44 percent). It is probably due to a new blade form based on data found in Reference 4 which resulted in an average rotor faction coefficient of $\lambda_f = 0.3$.

V. FUTURE WORK

While it was possible to obtain very good correlation of test data to the simplified theory, this theory is still only a first-order approximation. It would be very useful to know the influence of the variation of the friction coefficient with the geometric parameters. Some work in this area is indicated.

With the design parameters available from this study, a true constant-velocity turbine can be constructed. It would be very instructive to build and test such a unit and thereby verify the predicted efficiency of 44 percent.

REFERENCES

1. Balje, O. E., "Drag Turbine Performance." Trans. ASME., Aug. 57, pg 1291 ff.

2. A Study of High Energy Level, Low Power Output Turbines, Sundstrand Turbo Report AMF/TD No. 1196, 9 April 1958. AD-161323

3. Balje, O. E., "Accessory Drive Turbines for Aircraft and Missiles," Aeronautical Engineering Review, vol. 15, No. 3, March 1956, pg 60 ff.

4. Jackson, E. A., Experiments to Determine the Best Shape and Number of Vanes for a GGG Pump Runner, Inst. Mech. Eng. Proc., 1956, pg 415 ff.

APPENDIX A

1. The flow equations in finite-difference form are:

Momentum Equation.

$$\frac{\Delta P}{\bar{\gamma}} + \frac{\bar{c}\Delta c}{g} = -\left[\lambda_s \frac{\bar{c}^2}{2g}\frac{\Delta a_s}{A} + \lambda_r \frac{(\overline{c-u})^2}{2g}\frac{\Delta a_r}{A}\right]$$

Energy Equation:

$$c_p \Delta t + \frac{\bar{c}\Delta c}{g} + \Delta W = 0$$

Work Equation:

$$\Delta W = \frac{u}{c}\lambda_r \frac{(\overline{c-u})^2}{2g}\frac{\Delta a_r}{A}$$

Equation of State

$$p = \gamma R t$$

Continuity Equation:

$$\dot{W} = \gamma A c$$

where the barred letters indicate mean values.

2. These equations must be solved by trial and error. Knowing the initial conditions and assuming a value of Δc, the energy equation is solved for Δt. This establishes t_2, p_2, and Δp from the equation of state. Substitution in the momentum equation yields a value for Δc which must be equal to the assumed value. In this manner, the periphery of the turbine is traversed.

APPENDIX B - DERIVATION OF MAXIMUM HYDRAULIC EFFICIENCY

1. It has been shown (Equation 10) that the hydraulic efficiency is given by

$$\eta_H = \frac{\int X \lambda_r \frac{(1-x)^2}{x^2} \frac{da_r}{A}}{\int \lambda_s \frac{1}{x^2} \frac{da_s}{A} + \int \lambda_r \frac{(1-x)^2}{x^2} \frac{da_r}{A}}$$

$$= \frac{\int \frac{(1-x)^2}{X} \frac{da_r}{A}}{\frac{\lambda_s}{\lambda_r} \int \frac{1}{x^2} \frac{da_s}{A} + \int \frac{(1-x)^2}{x^2} \frac{da_r}{A}}$$

For the constant-velocity case this reduced to (Equation 29)

$$(\eta_H)_c = \frac{X}{\frac{\delta_{eq}}{(1-x)^2} + 1}$$

and the maximum efficiency is shown in Figure B-1.

2. For the constant-area case

$$(\eta_H)_A = \frac{\int \frac{(1-x)^2}{X} d\theta}{\delta_{eq}' \int \frac{d\theta}{x^2} + \int \frac{(1-x)^2}{x^2} d\theta}$$

where

$$\delta_{eq}' = \frac{k_s \lambda_s}{k_r \lambda_r}$$

It is possible to solve for the efficiency if the velocity variation is assumed. Two cases have been investigated, i.e.,

$$C = C_1 + \alpha\Theta$$

and

$$C = C_1 e^{\beta\Theta}$$

It is realized that the velocity may not fit either equation exactly, but, at least, a qualitative feeling for the efficiency variation is possible. The result of the integration shows that the efficiency is a function of the ratio of initial to final velocity which, by the continuity equation, equals the density ratio

$$\frac{C_f}{C_1} = \frac{\gamma_1}{\gamma_f} = \frac{X_1}{X_f}$$

where

$$X = \frac{U}{C}$$

In the case of the linear velocity variation, the efficiency is

$$(\eta_H)_{\substack{A \\ C=C_1+\alpha\Theta}} = \frac{\ln\frac{\gamma_1}{\gamma_f} + \frac{1}{2}X_1^2\left[1-\frac{1}{(\gamma_1/\gamma_f)^2}\right] - 2X_1\left[1-\frac{1}{\gamma_1/\gamma_f}\right]}{-2\ln\frac{\gamma_1}{\gamma_f} + \left(1+\delta_{eq}'\right)\frac{1}{X_1}\left[\frac{\gamma_1}{\gamma_f}-1\right] + X_1\left[1-\frac{1}{\gamma_1/\gamma_f}\right]}$$

which is Equation 22 of Ref. 1.

For the exponential distribution

$$(\eta_H)_{A \atop C=C_1 e^{\beta\Theta}} = \frac{\frac{1}{X_1}\left[\frac{\gamma_1}{\gamma_t} - 1\right] - 2\ln\frac{\gamma_1}{\gamma_t} + X_1\left[1 - \frac{1}{\gamma_1/\gamma_t}\right]}{\frac{(1+\delta_{eq}')}{2}\ \frac{1}{X_1^2}\left[\left(\frac{\gamma_1}{\gamma_t}\right)^2 - 1\right] + \ln\frac{\gamma_1}{\gamma_t} - \frac{2}{X_1}\left[\frac{\gamma_1}{\gamma_t} - 1\right]}$$

The maximum efficiency for these two cases is shown in Figure B-2. It is somewhat surprising to find that very little difference exists between the two which leads to the conclusion that the efficiency is relatively unaffected by the exact expression for the velocity distribution.

NOMENCLATURE

a	surface area (in.^{2})
A	throughflow area (in.^{2})
b	throughflow channel height (in.)
c_p	specific heat at constant pressure (ft-lb/lb°)
c	throughflow velocity (fps)
c_o	spouting velocity (fps)
d	rotor root diameter (in.)
D	rotor tip diameter (in.)
D	Drag (lbs)
e	blade height (in.)
f	tip clearance (in.)
g	gravitational constant - 32.2 ft/sec^2
H	head (ft)
H	side-channel depth (in.)
H'	blade width (in.)
k	constant
m	H'/H
p	pressure (psf)
Q	heat flow (ft-lb/lb)
r	radius (in.)

NOMENCLATURE (continued)

t	temperature (°R)
u	wheel peripheral velocity, mean (fps)
$\dot{w}$	weight-flow rate (lbs/sec)
W	work (ft-lb/lb)
x	velocity ratio, u/c
Y	$\frac{b-e}{H} = \frac{f}{H}$
γ	density (lb/ft^3)
ε	$\frac{2r_m + e}{2r_m - e}$
η	efficiency
θ	rotor angle
κ	ratio of specific heats
λ	friction factor
τ	shear stress (psi)

Subscripts

$()_{ad}$	adiabatic
$()_H$	hydraulic
$()_r$	rotor
$()_s$	stator

TABLE I

LIST OF TEST INSTRUMENTATION

Symbol	Instrument	Source	Range	Accuracy
$\triangle p_o$	Flow meter	Barton		ASME power test code
	$\triangle$p gage	Barton	0 ±25 psi 0.5 psi grad.	0.5% full scale
p_E	Flow meter	Daniel		ASME power test code
	Manometer	Meriam	0-100" H_2O	
p_o	Inlet orifice gage	Norden Ketay	0-200 psi	1% F.S.
p_1 through p_9	Gages	Acragage	0-160 psi 0-100 psi 0-60 psi	1% F.S.
p_E	Exhaust orifice manometer	Trimount	0-60 in. Hg	
t	Thermocouples - total, copper const.		-100 to +500 °F	
	Potentiometer - indicating 40 point		-200 to +200 °F	.25%
Torque	Force ring	Wiancko Eng	± 20 lbs	0.5%
	Carrier oscillator	Wiancko Eng		
	Demodulator	Wiancko Eng		
	Ammeter	Simpson	0-100 in. lbs	1% F.S.
RPM	Magnetic pickup		2 pulses/rev	
	Electronic counter	Hewlett Packard	0-99,999 cps	0.1%

ILLUSTRATIONS

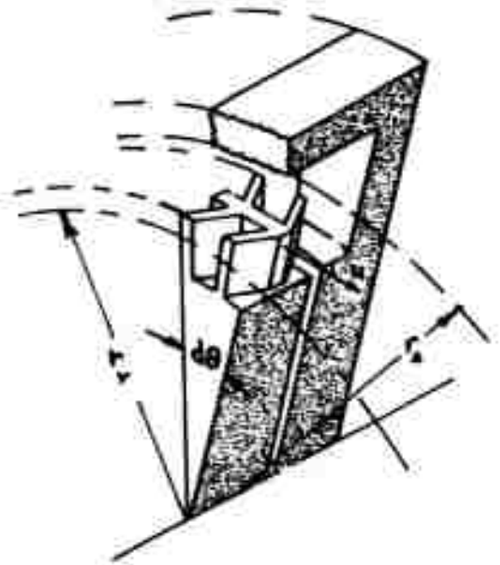

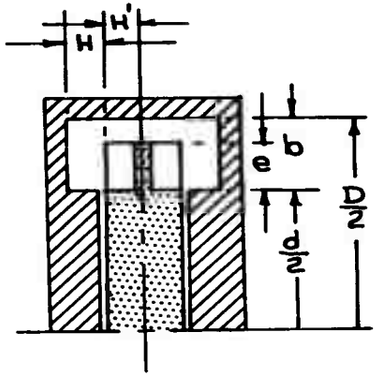

$$A = 2b(H+H') - 2eH'$$

$$da_r = (r_r\, d\theta)h$$

$$da_s = (r_s\, d\theta)n$$

where

$$h = k'_r(H'+e)$$

$$n = k'_s(H+H'+b)$$

$$r_r = \frac{d}{2} + \frac{e}{2}$$

$$r_s = \frac{d}{2} + \frac{b}{2}$$

DEFINITION OF AREAS

FIGURE 1.

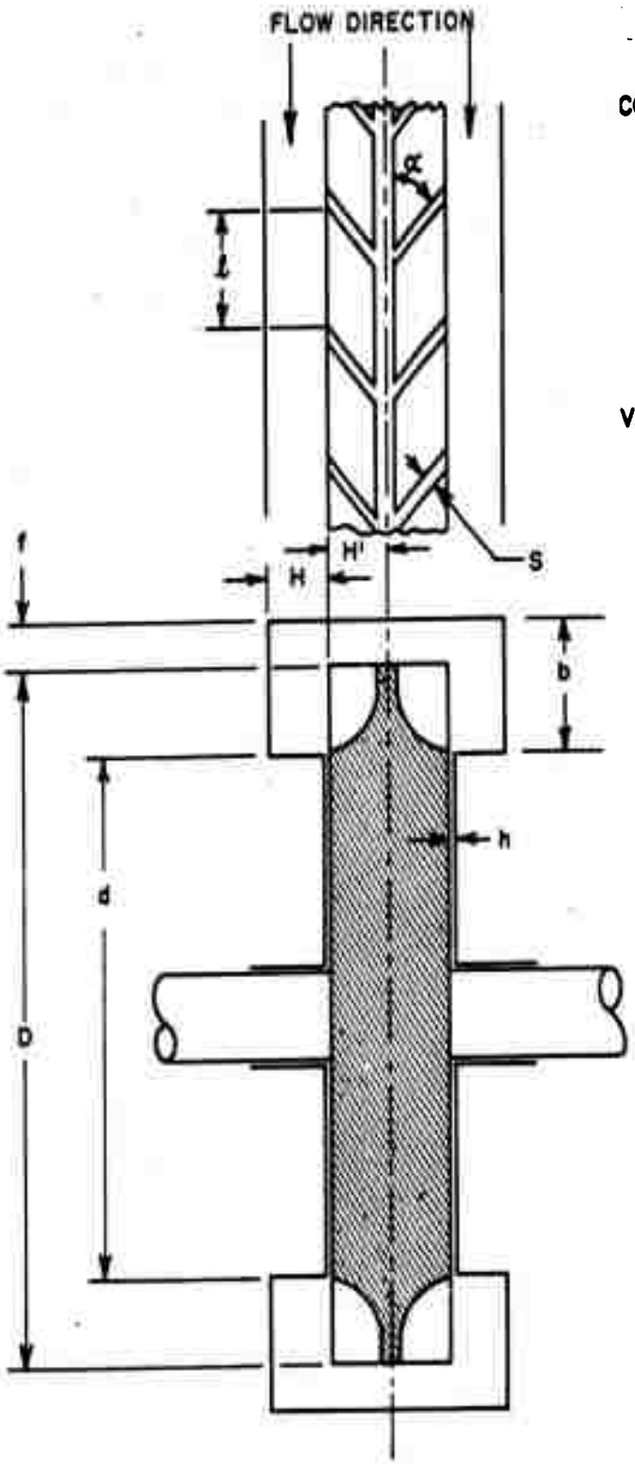

CONSTANTS:

- α ≅ 35°
- S ≅ .030 in.
- $\mathcal{L}$ ≅ .240 in.
- D ≅ 3.000 in.
- d ≅ 2.492 in.
- h ≅ .003 in
- H' ≅ .174 in.

VARIABLES:

angular location	H in.	f in.
45°	.145	.014
122°	.151	.024
201°	.164	.058
280°	.200	.130

FIGURE 2.
OUTSIDE DIVERGENT CHANNEL DESIGN

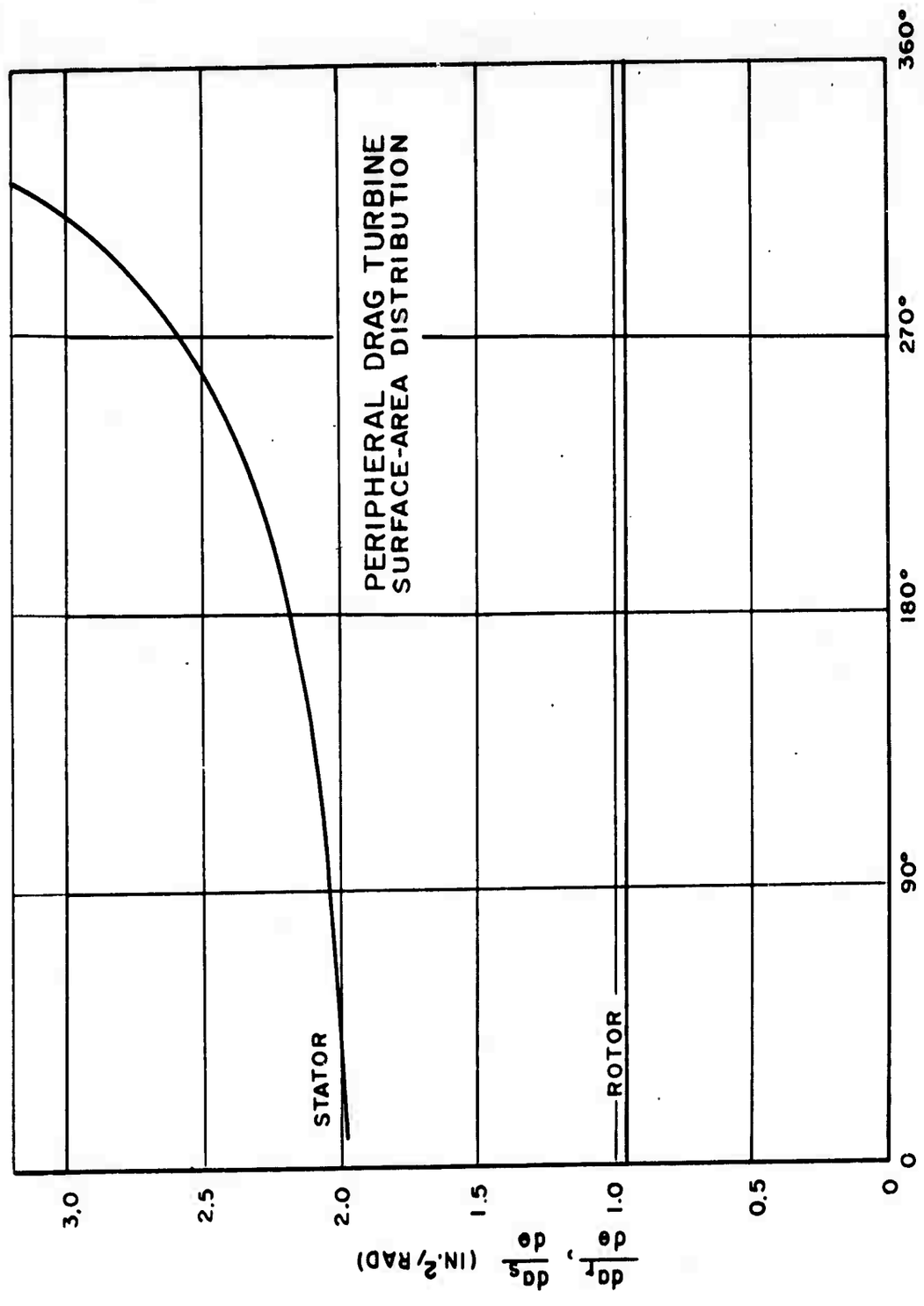
PERIPHERAL DRAG TURBINE
SURFACE-AREA DISTRIBUTION
STATOR
ROTOR
3.0
2.5
2.0
1.5
1.0
0.5
0
0°
90°
180°
270°
360°
ANGULAR POSITION
$\frac{dA_r}{d\theta}, \frac{dA_s}{d\theta}$ (IN.²/RAD)

FIGURE 3.

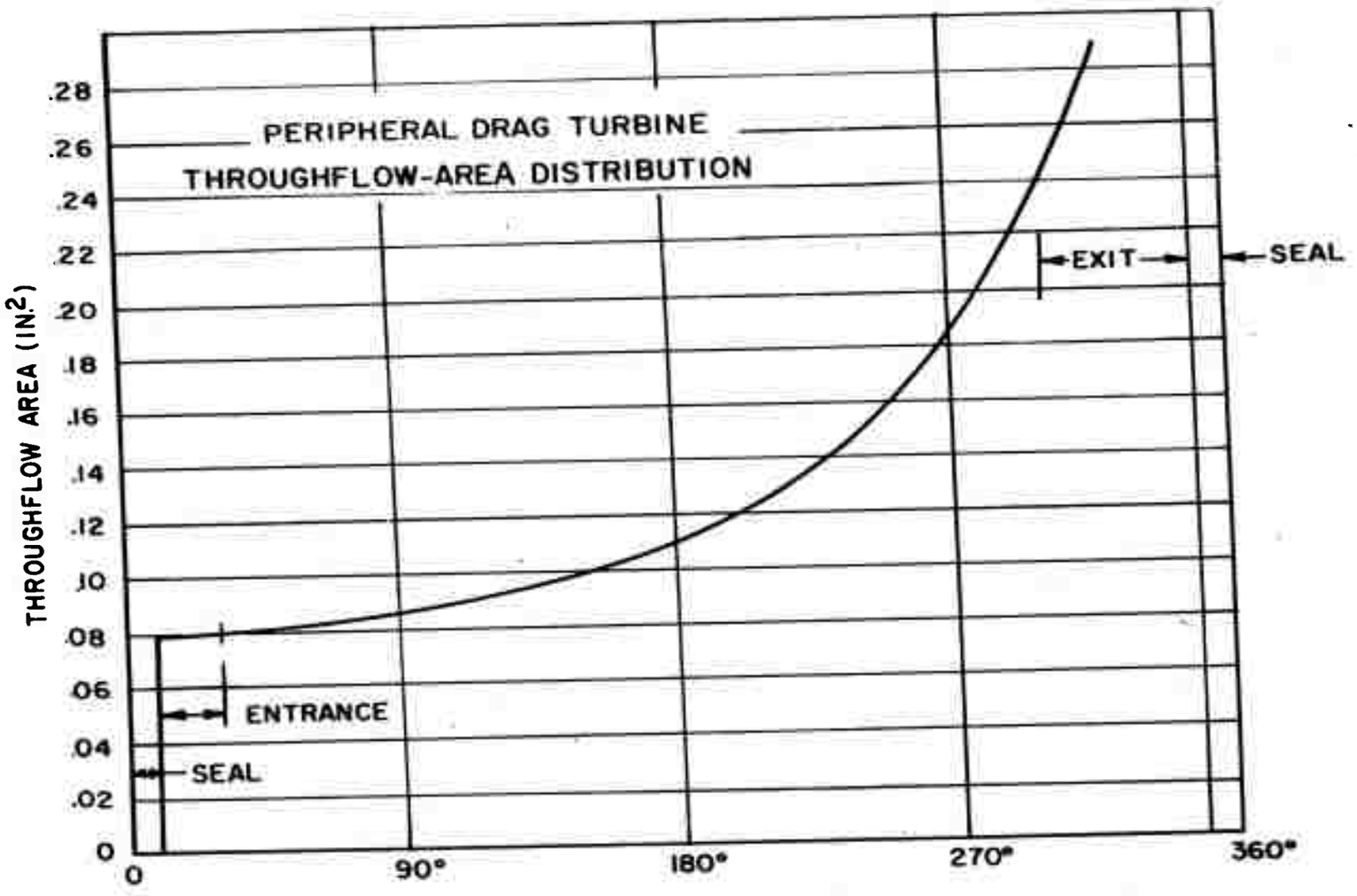

FIGURE 4.

SUNDSTRAND TURBO

DIVISION OF SUNDSTRAND CORPORATION

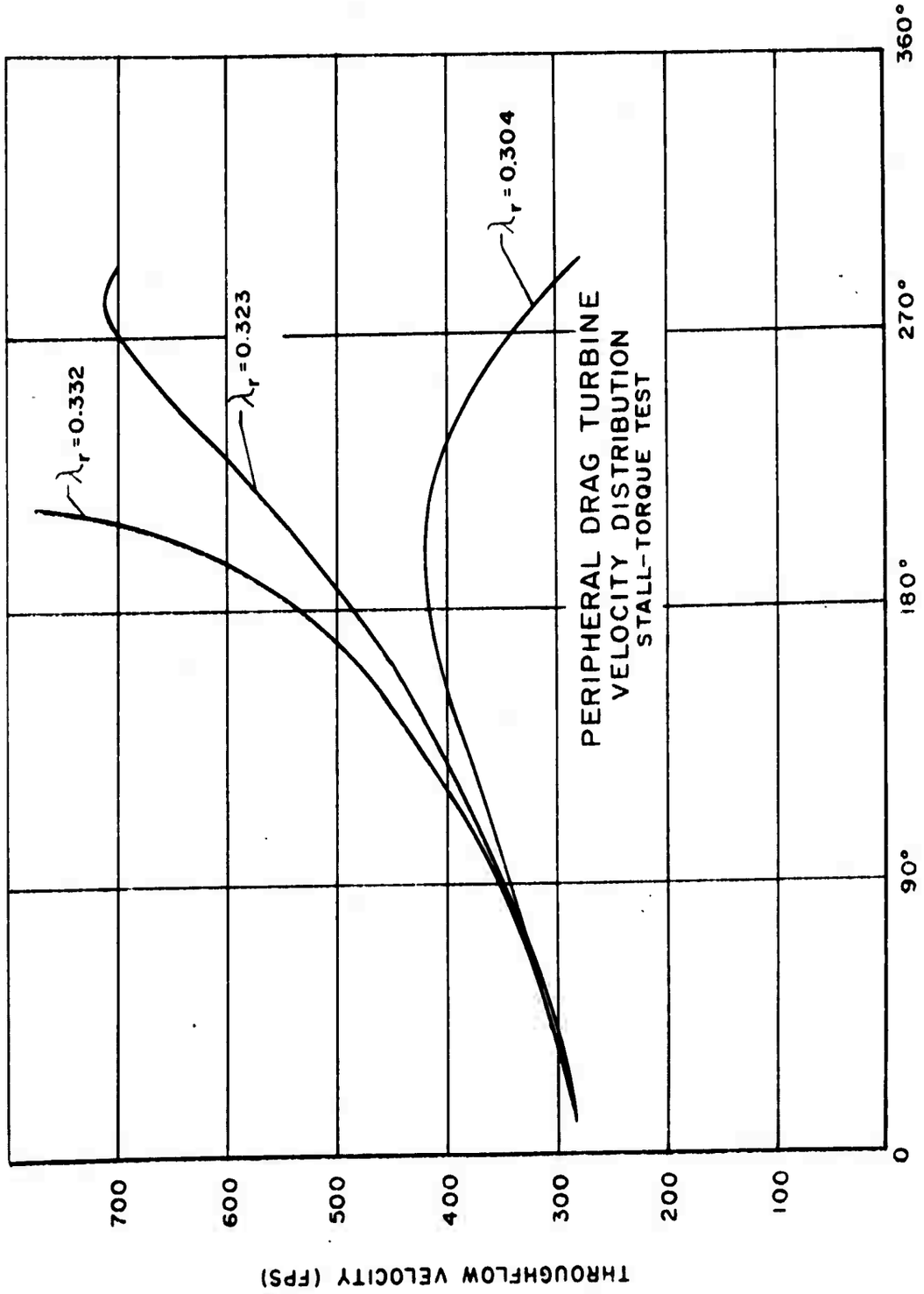
PERIPHERAL DRAG TURBINE
VELOCITY DISTRIBUTION
STALL-TORQUE TEST
$\lambda_r = 0.332$
$\lambda_r = 0.323$
$\lambda_r = 0.304$
THROUGHFLOW VELOCITY (FPS)
700
600
500
400
300
200
100
0
90°
180°
270°
360°
ANGULAR POSITION (°)

FIGURE 5

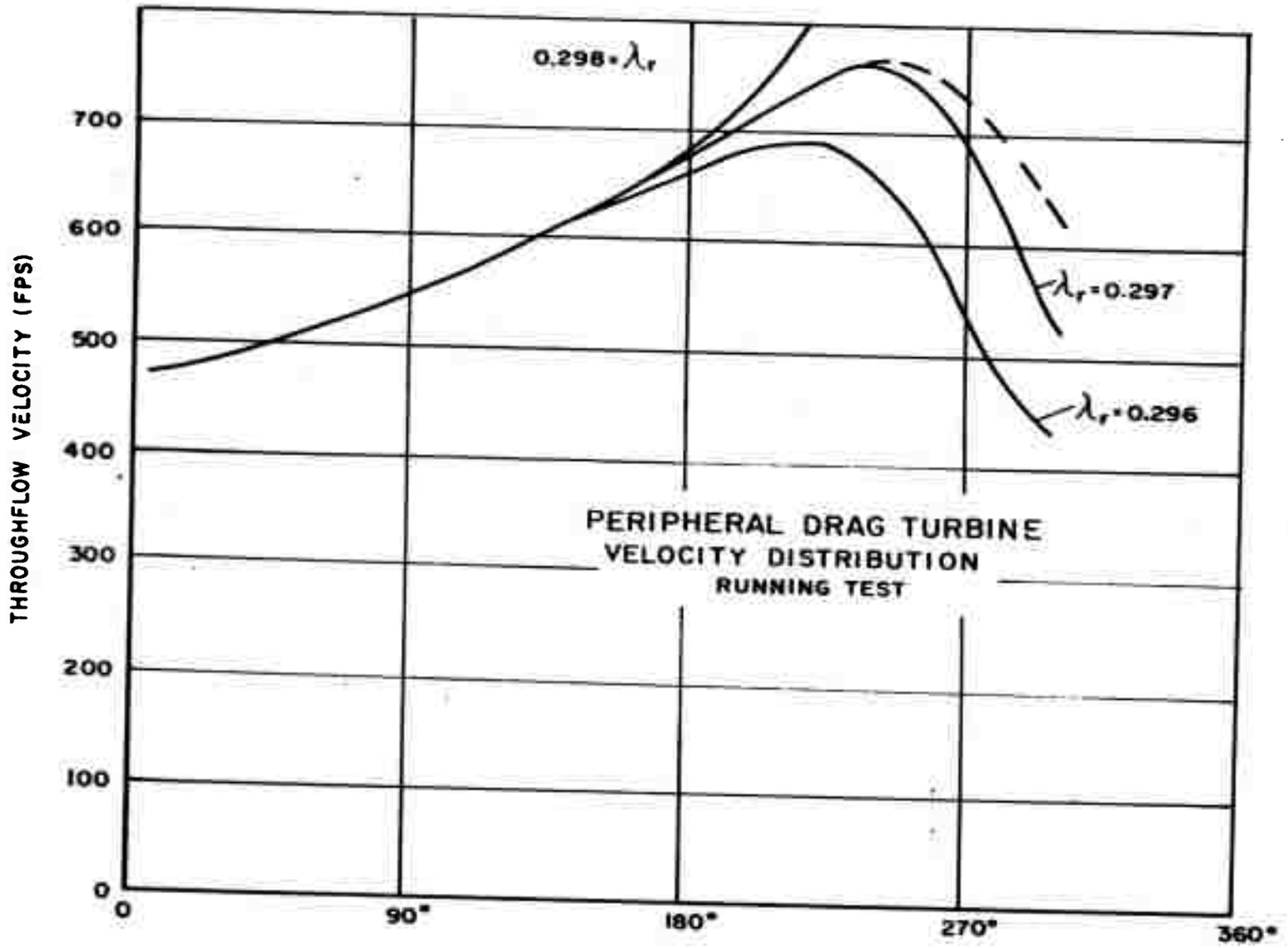

FIGURE 6.

SUNDSTRAND TURBO

DIVISION OF SUNDSTRAND CORPORATION

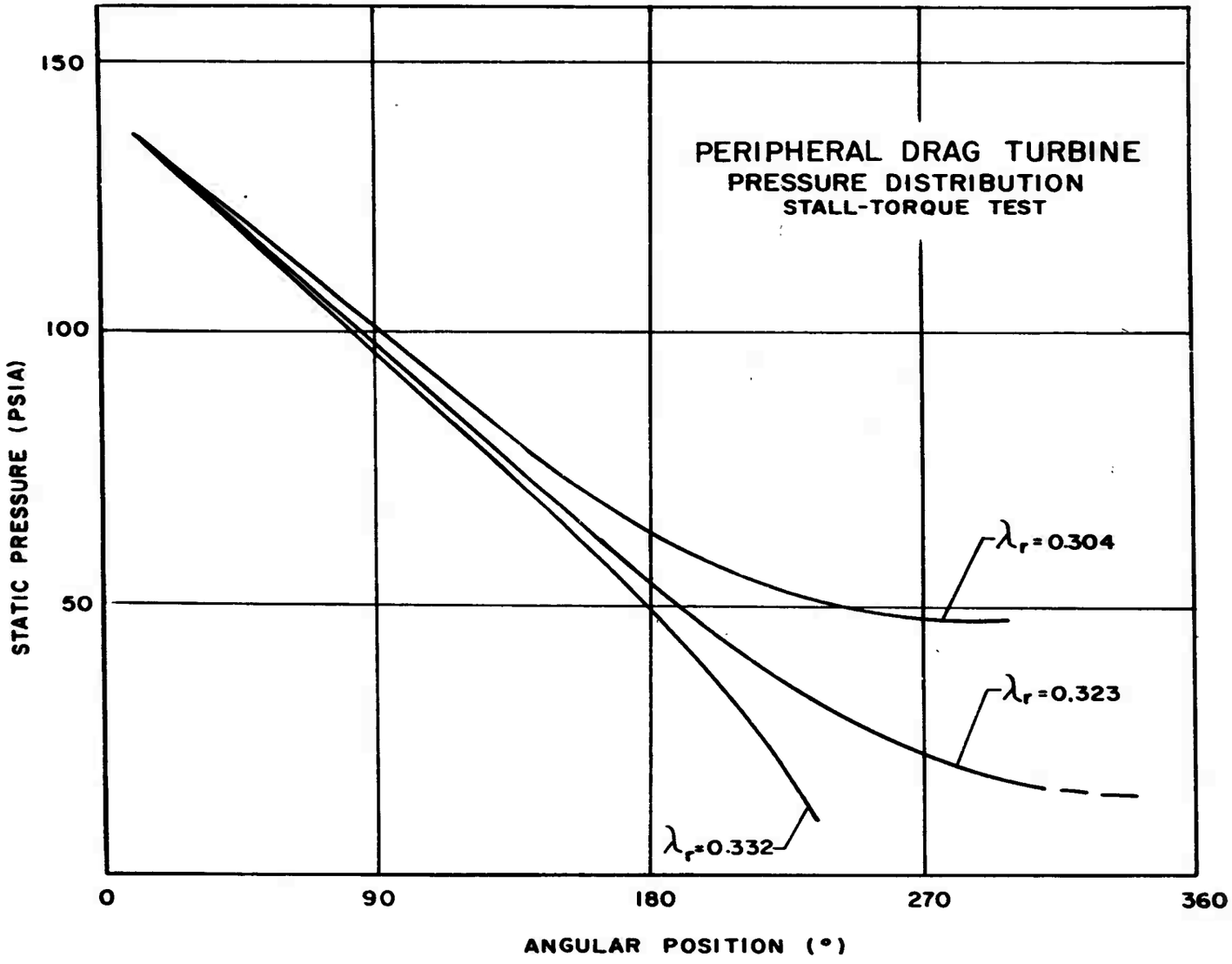

FIGURE 7.

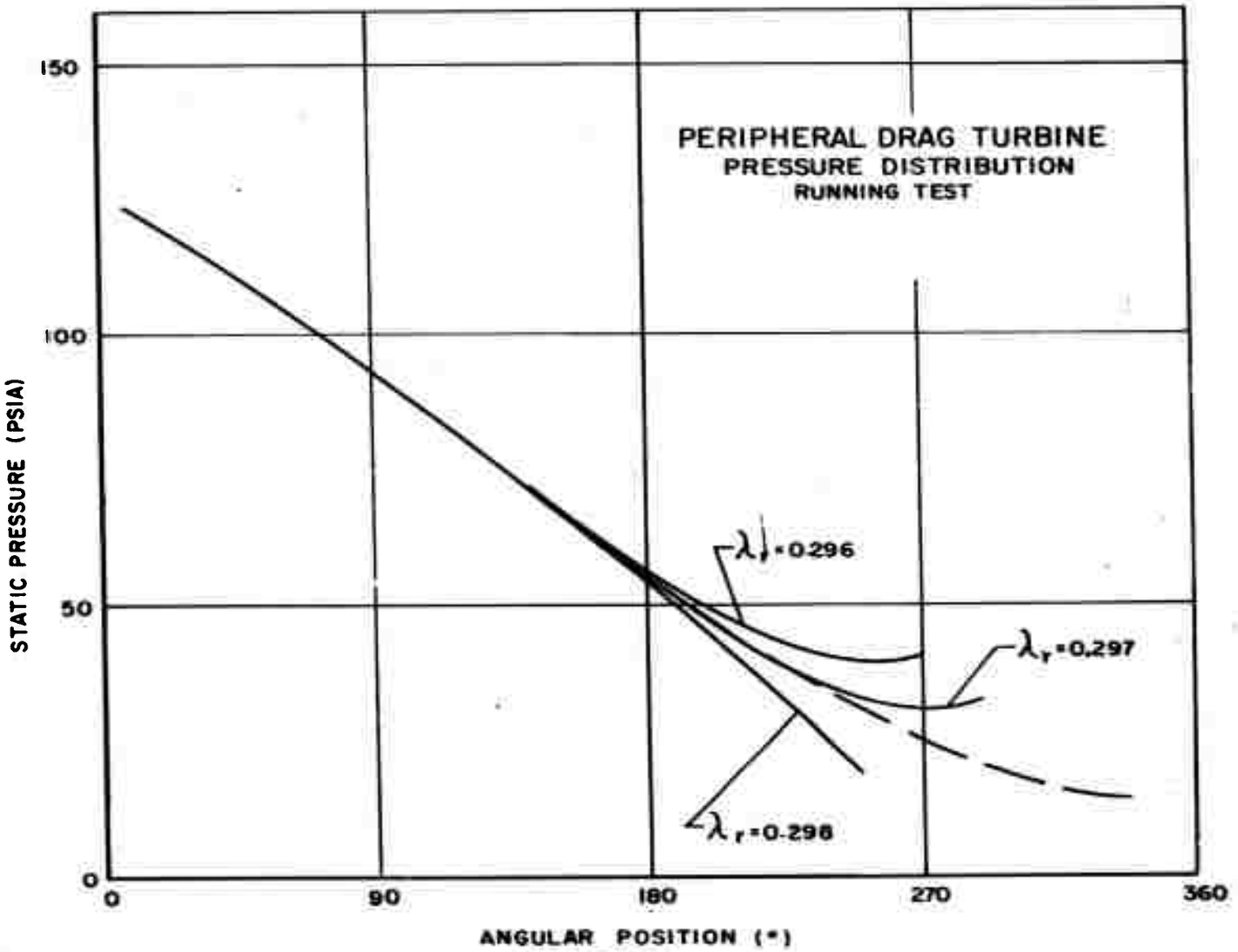
PERIPHERAL DRAG TURBINE
PRESSURE DISTRIBUTION
RUNNING TEST
STATIC PRESSURE (PSIA)
150
100
50
0
0
90
180
270
360
ANGULAR POSITION (°)
λ_r=0.296
λ_r=0.297
λ_r=0.298

FIGURE 8.

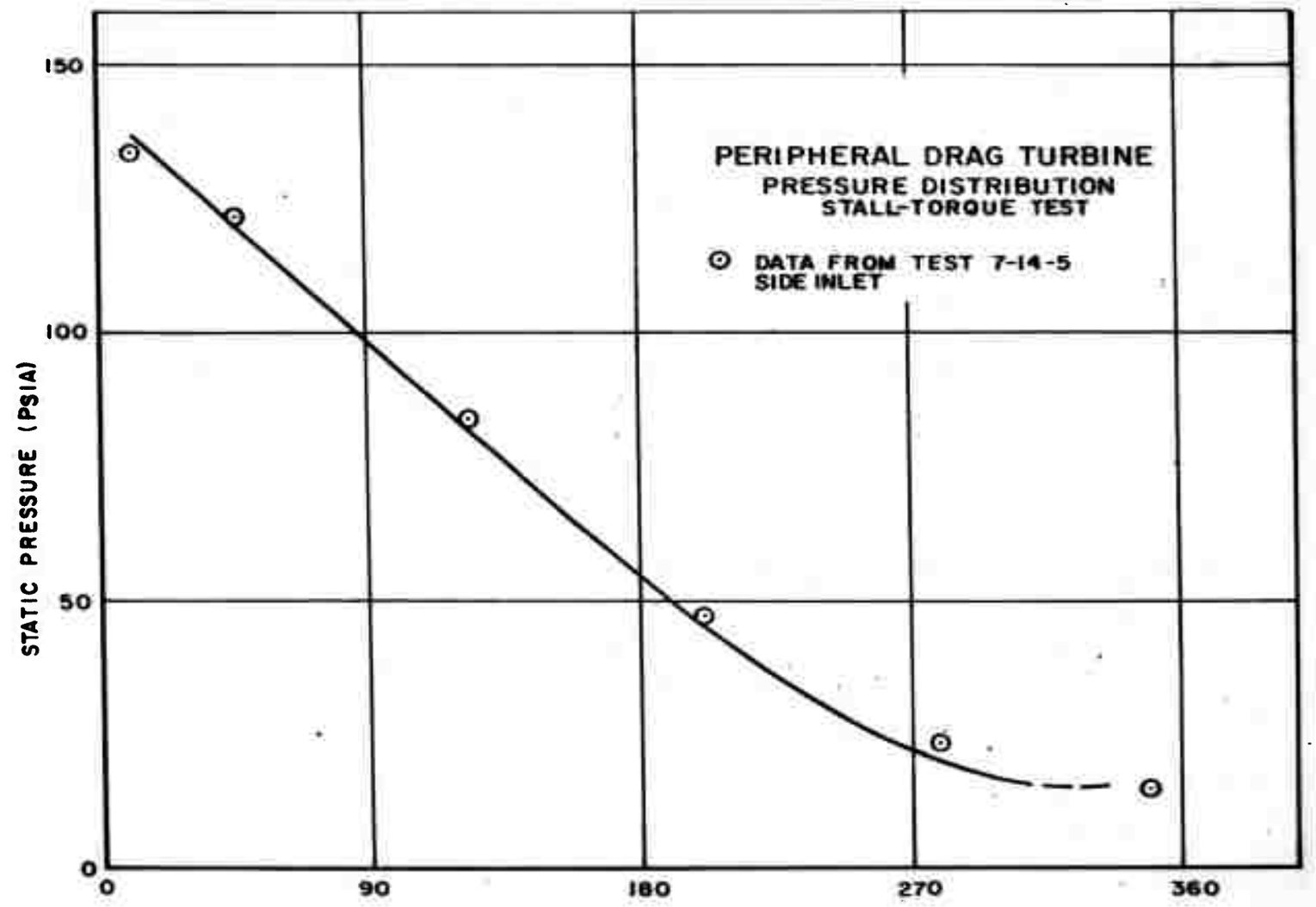

FIGURE 9.

SUNDSTRAND TURBO

DIVISION OF SUNDSTRAND CORPORATION

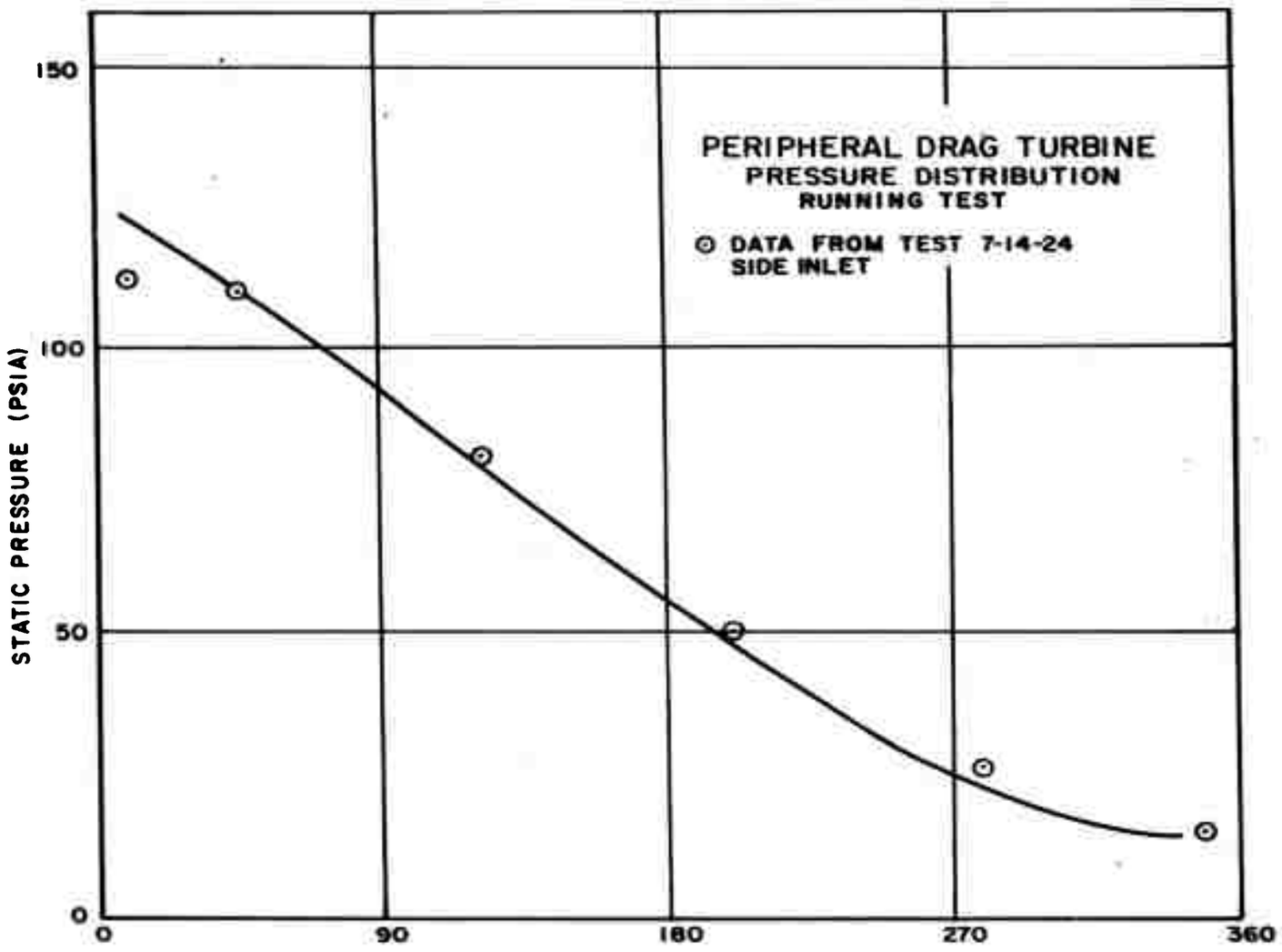

FIGURE 10.

SUNDSTRAND TURBO

DIVISION OF SUNDSTRAND CORPORATION

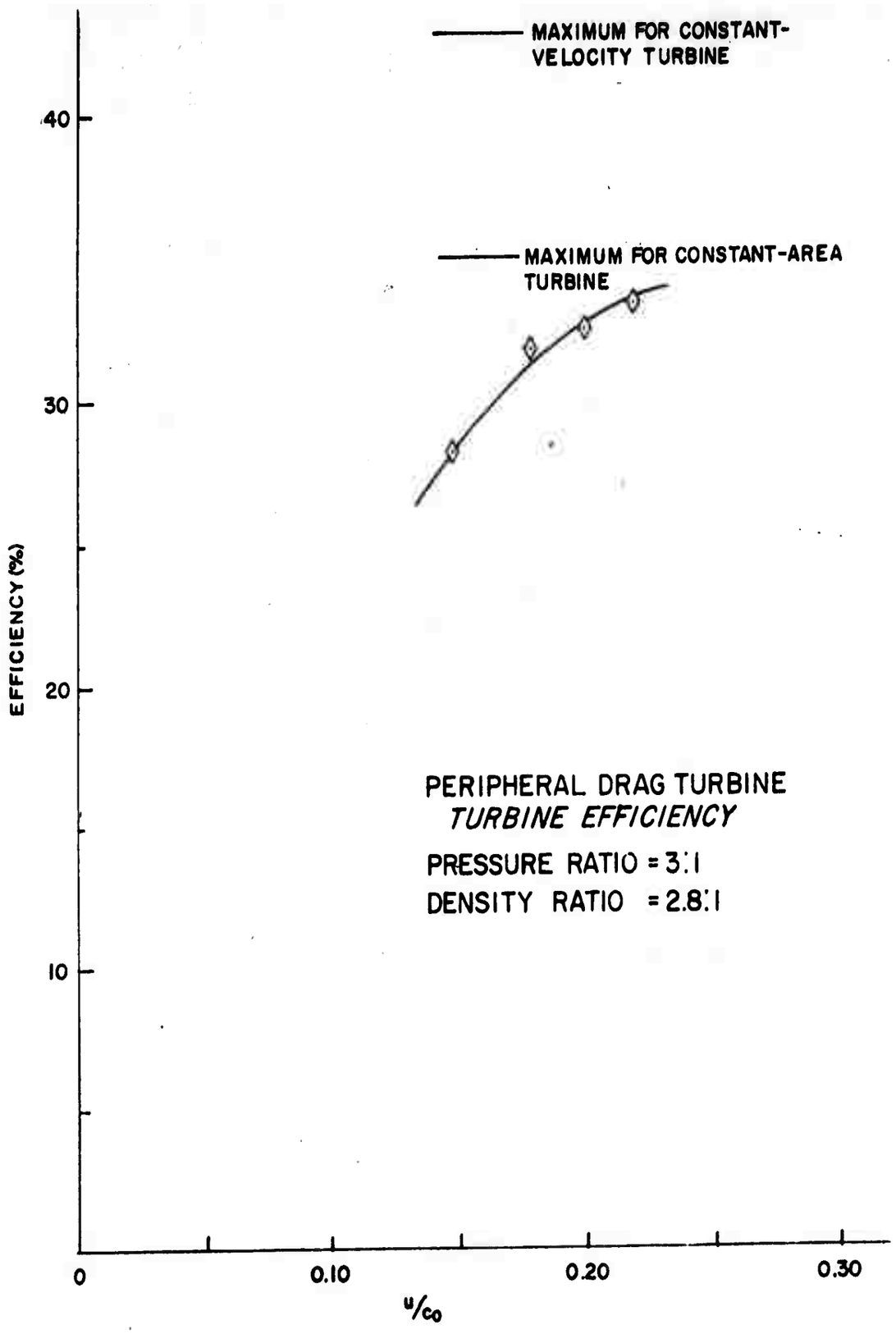

FIGURE 11.

SUNDSTRAND TURBO

DIVISION OF SUNDSTRAND CORPORATION

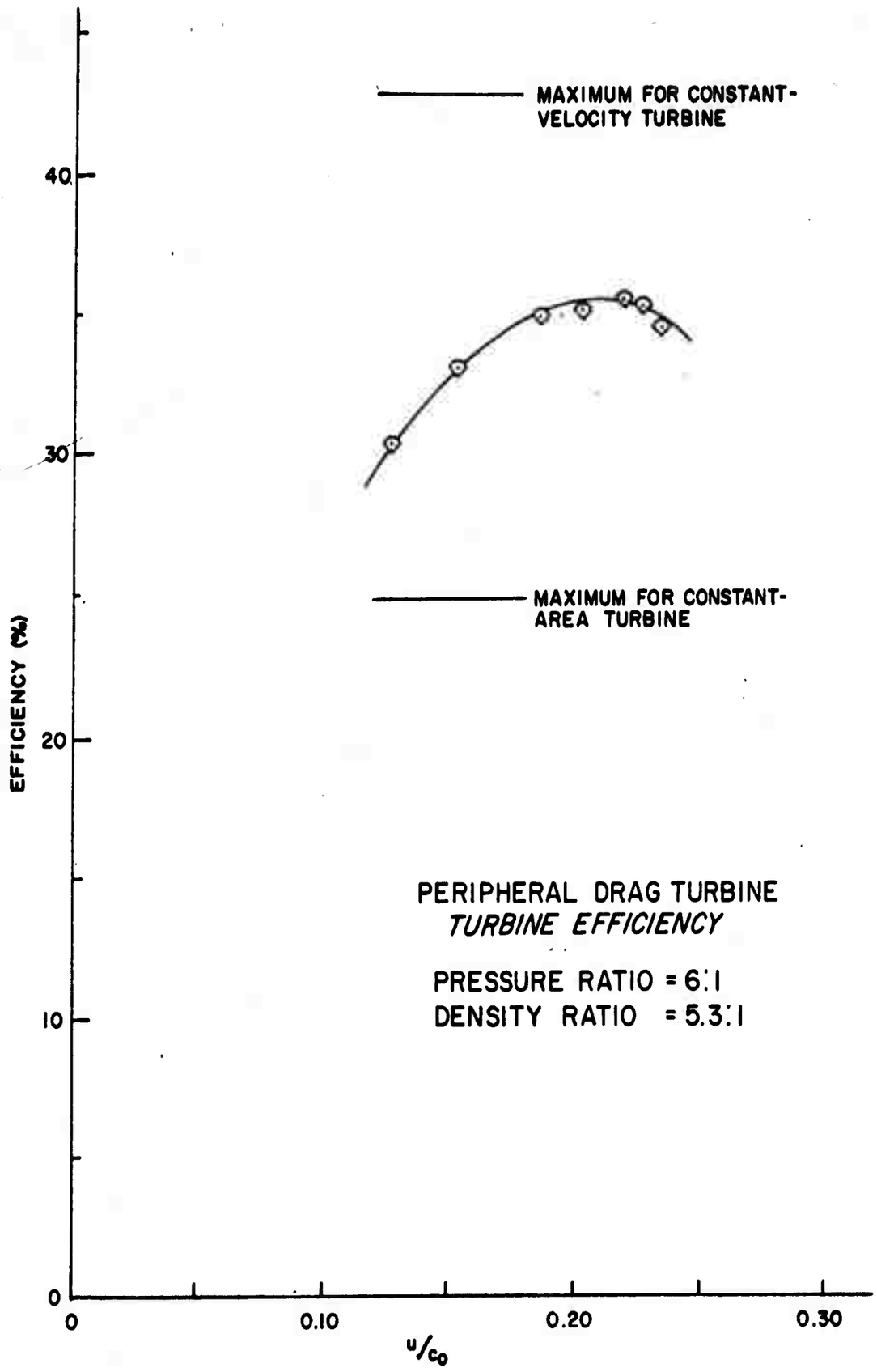

FIGURE 12.

SUNDSTRAND TURBO

DIVISION OF SUNDSTRAND CORPORATION

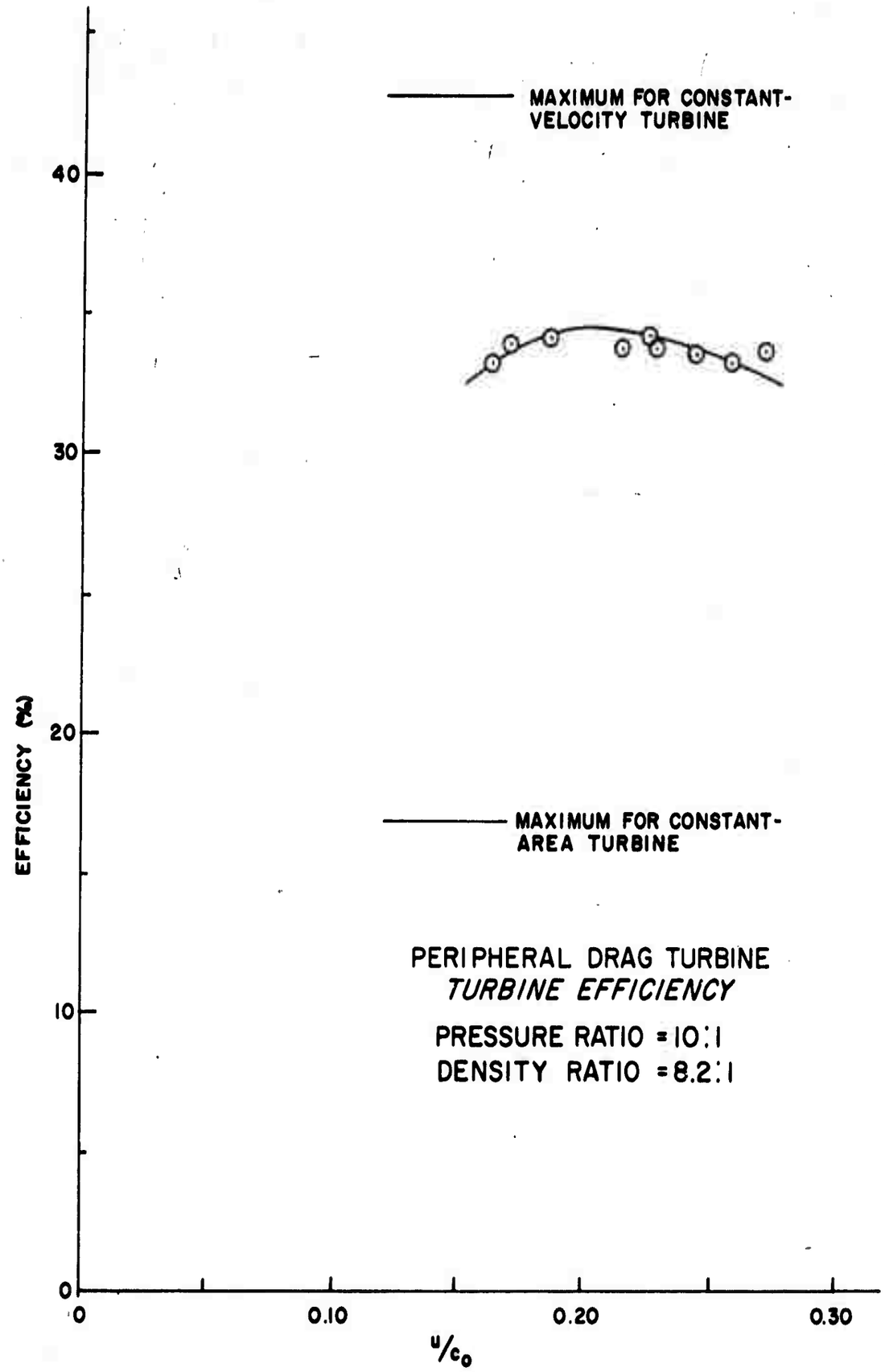

FIGURE 13.

SUNDSTRAND TURBO

DIVISION OF SUNDSTRAND CORPORATION

STATOR GEOMETRY
SIDE INLET & EXHAUST

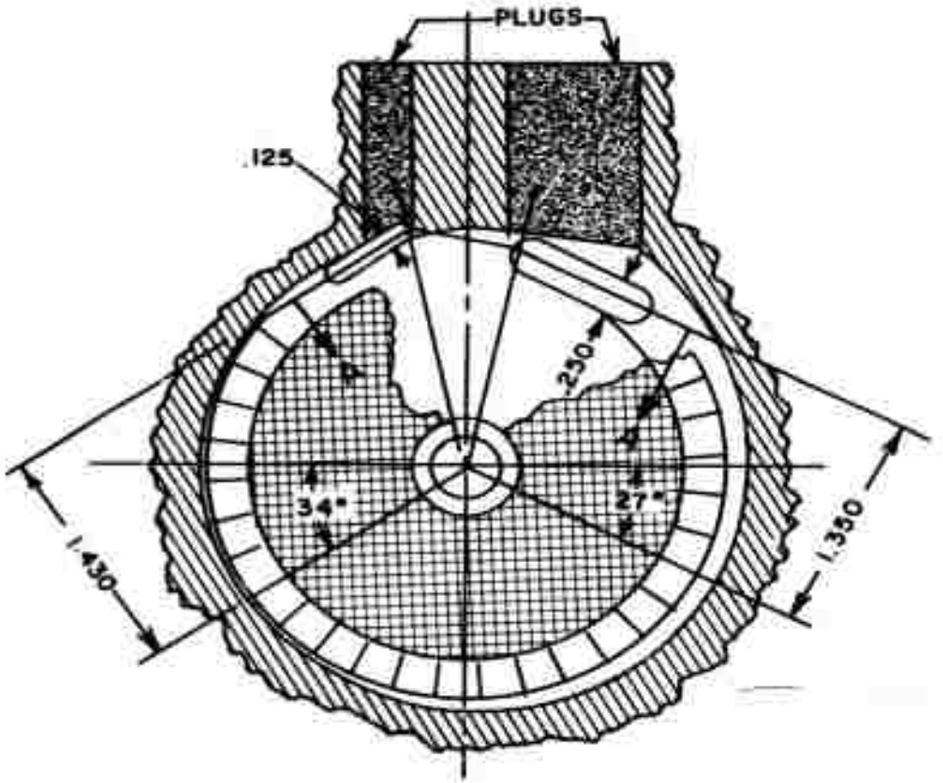

SECTION BB

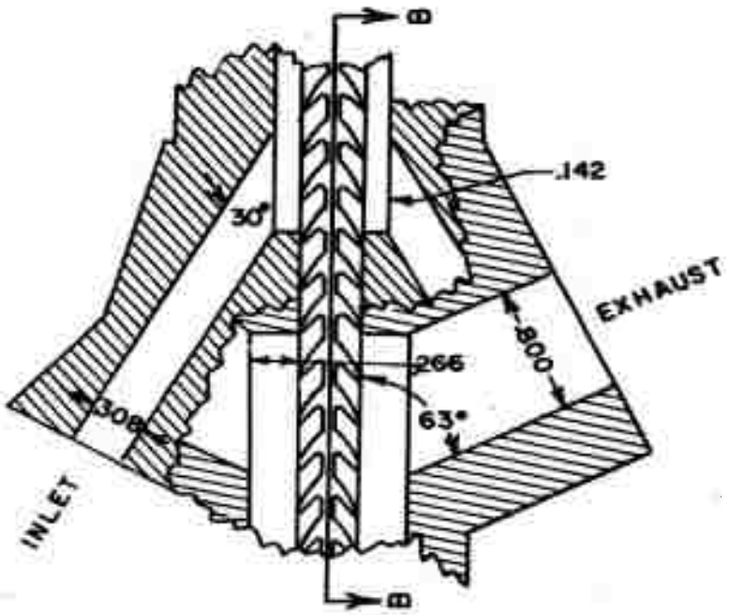

SECTION AA

FIGURE 14.

STATOR GEOMETRY
TOP INLET AND EXHAUST

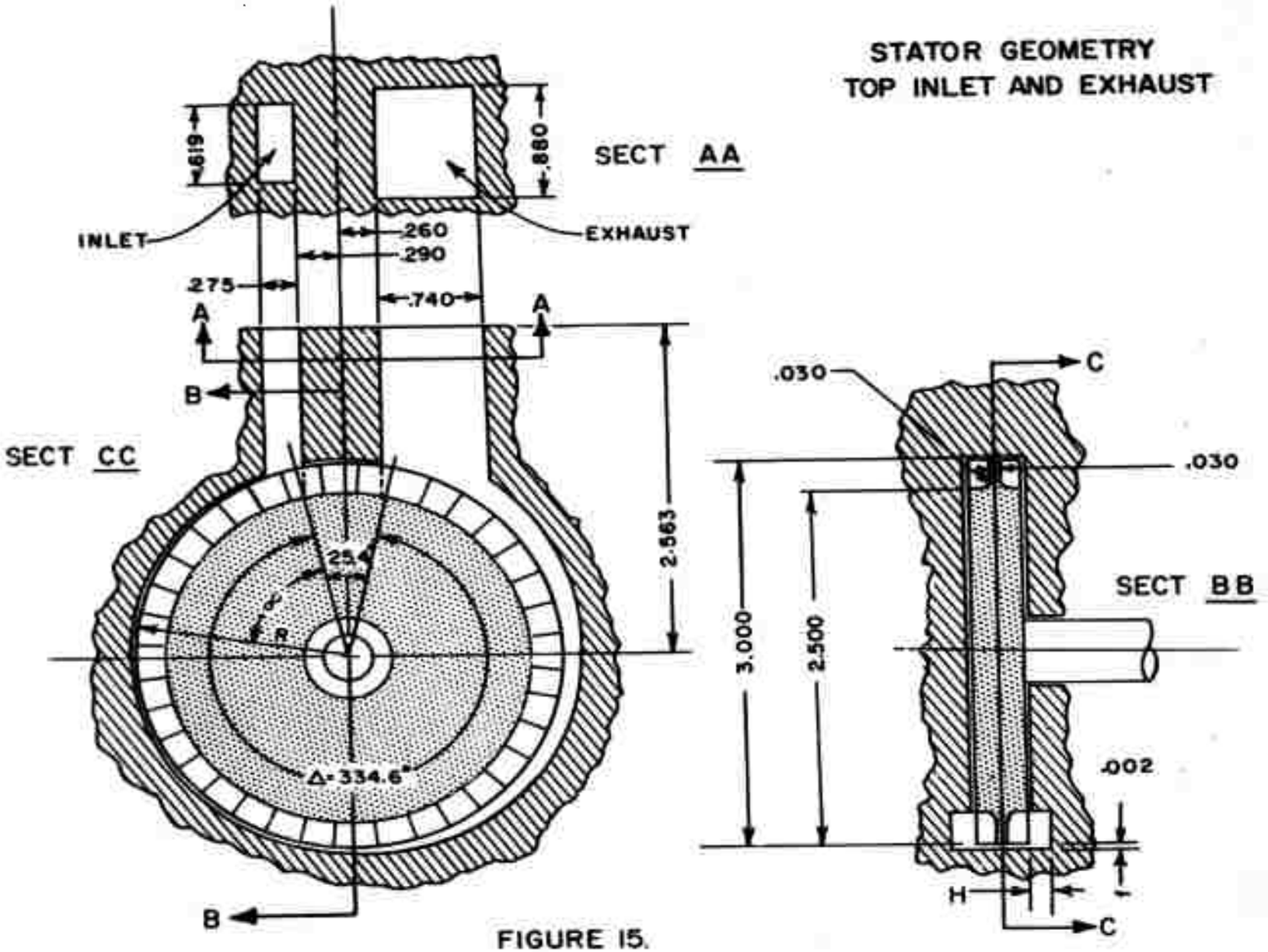

FIGURE 15.

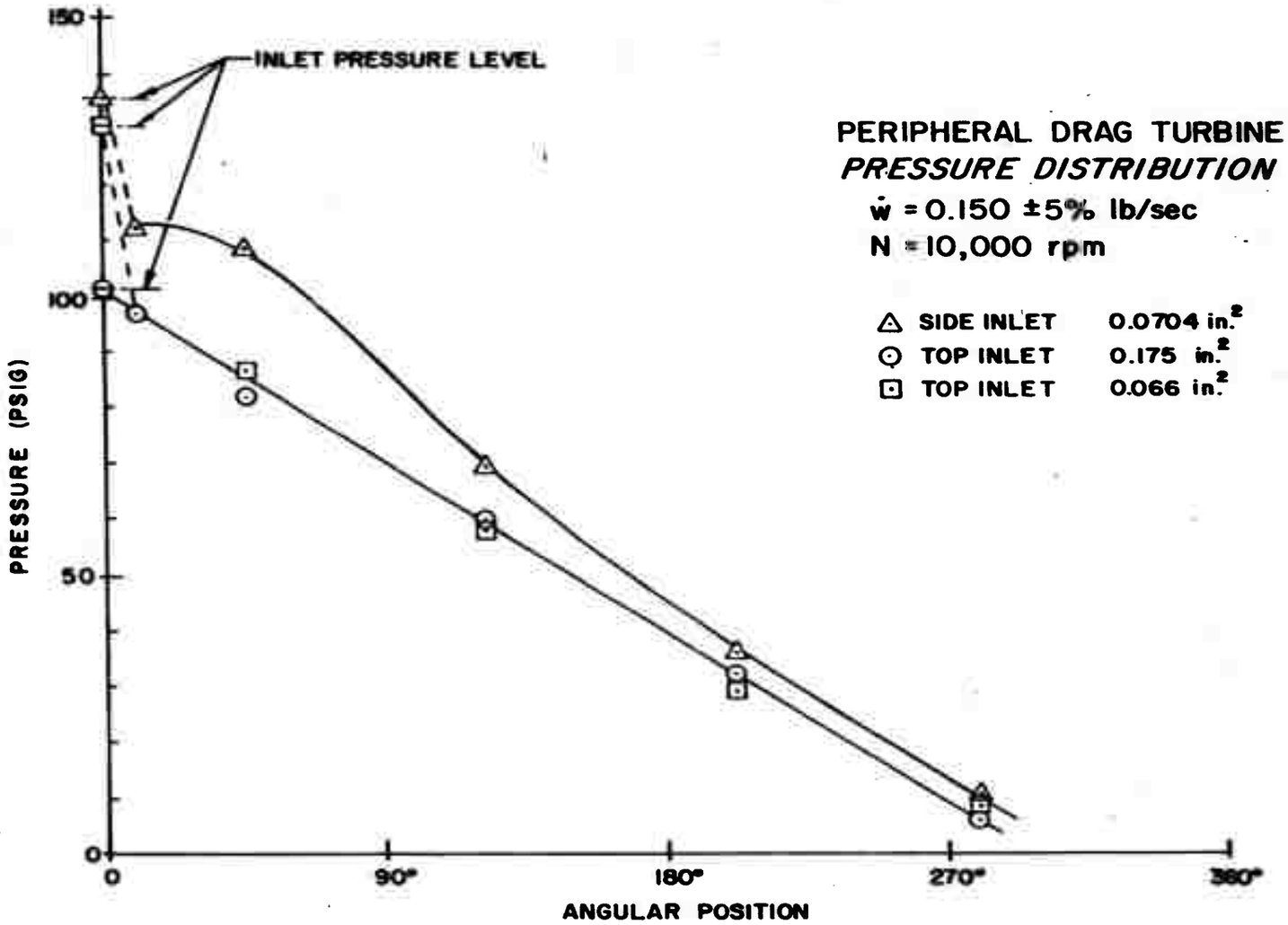

FIGURE 16.

SUNDSTRAND TURBO

DIVISION OF SUNDSTRAND CORPORATION

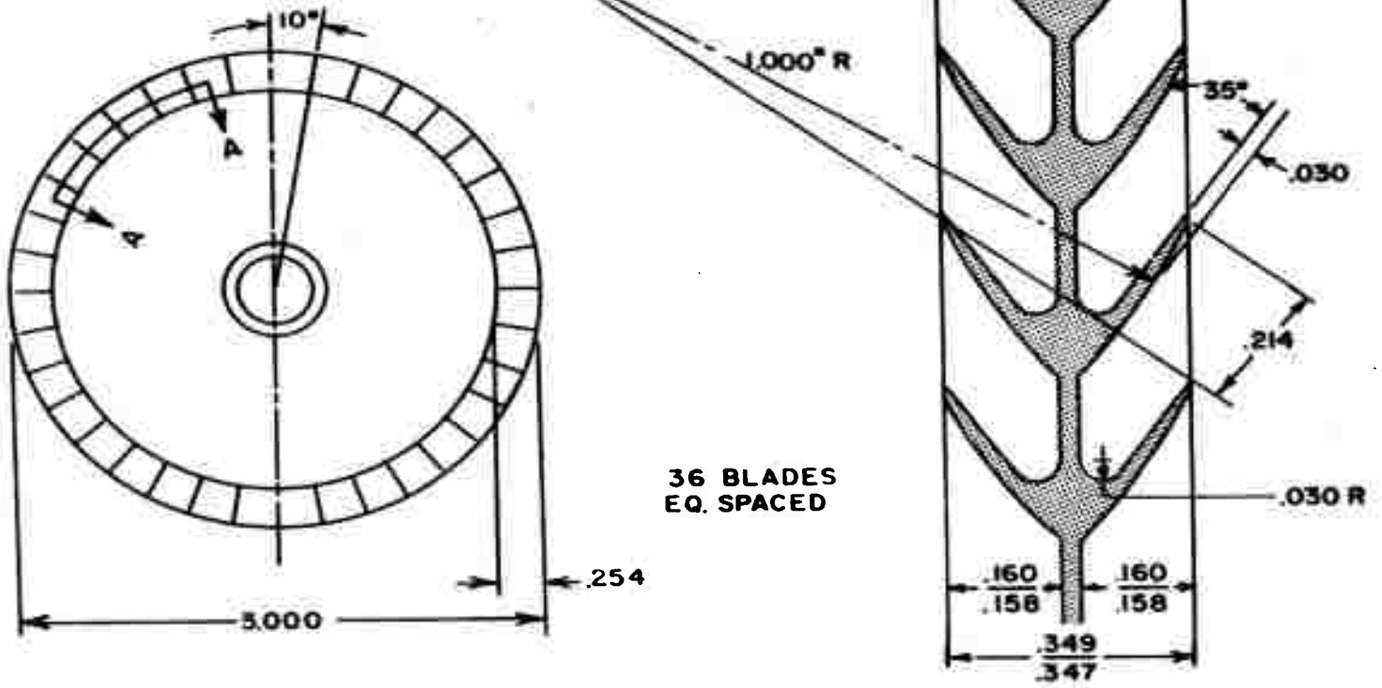

ROTOR GEOMETRY

FIGURE 17.

Figure 18. Control Room - Turbine Laboratory

Figure 19. Control Console - Turbine Laboratory

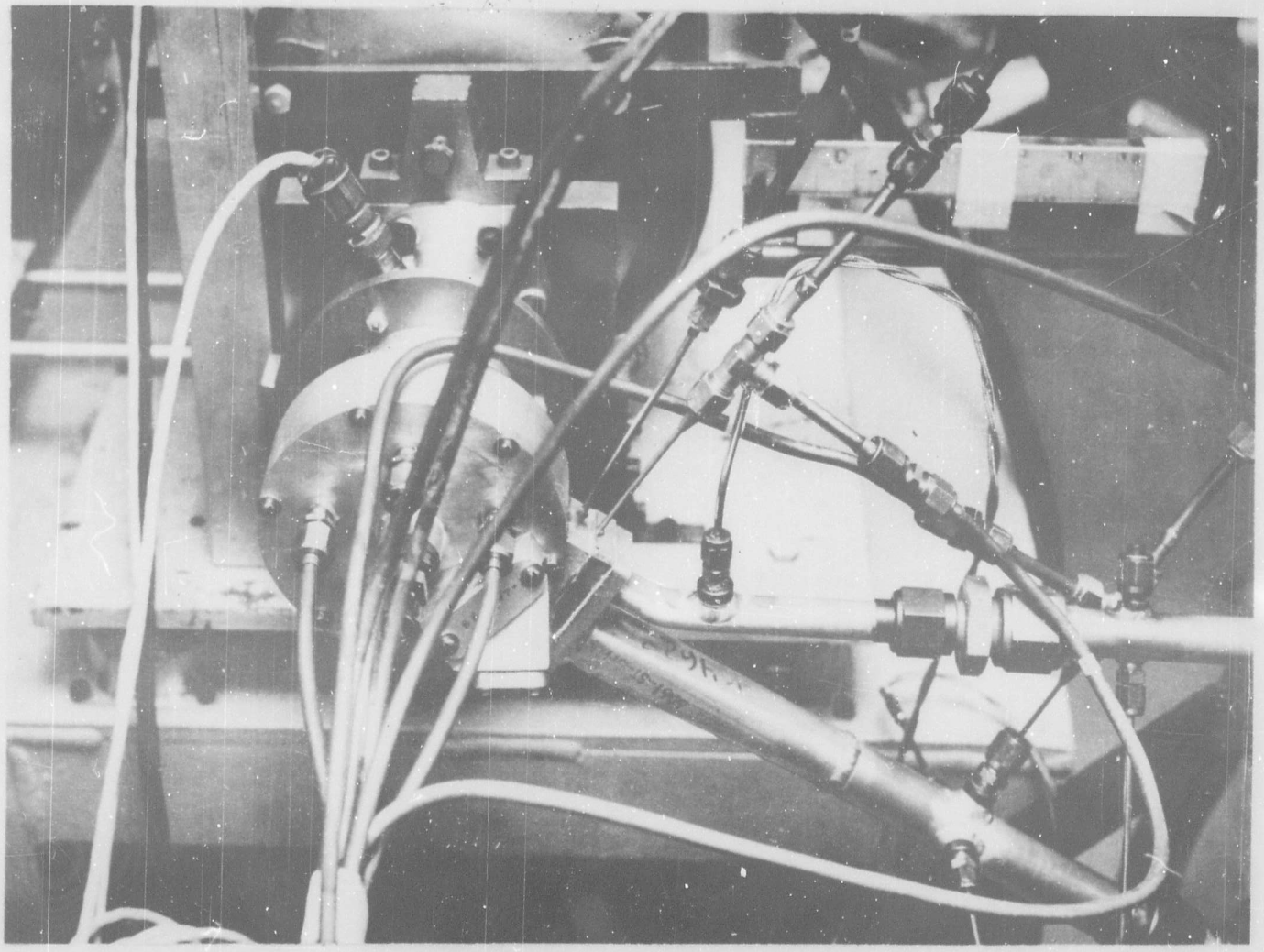

Figure 20. Turbine Test Stand

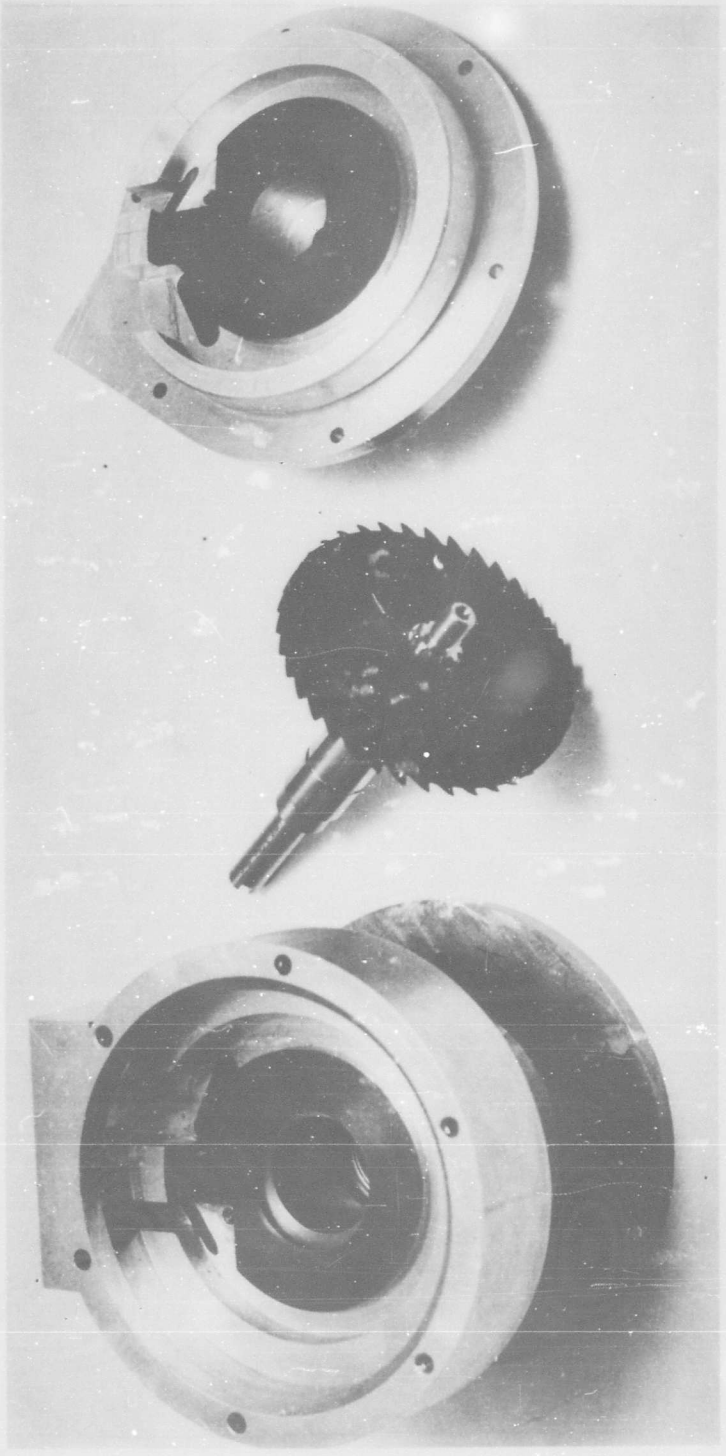

Figure 21. Turbine Components

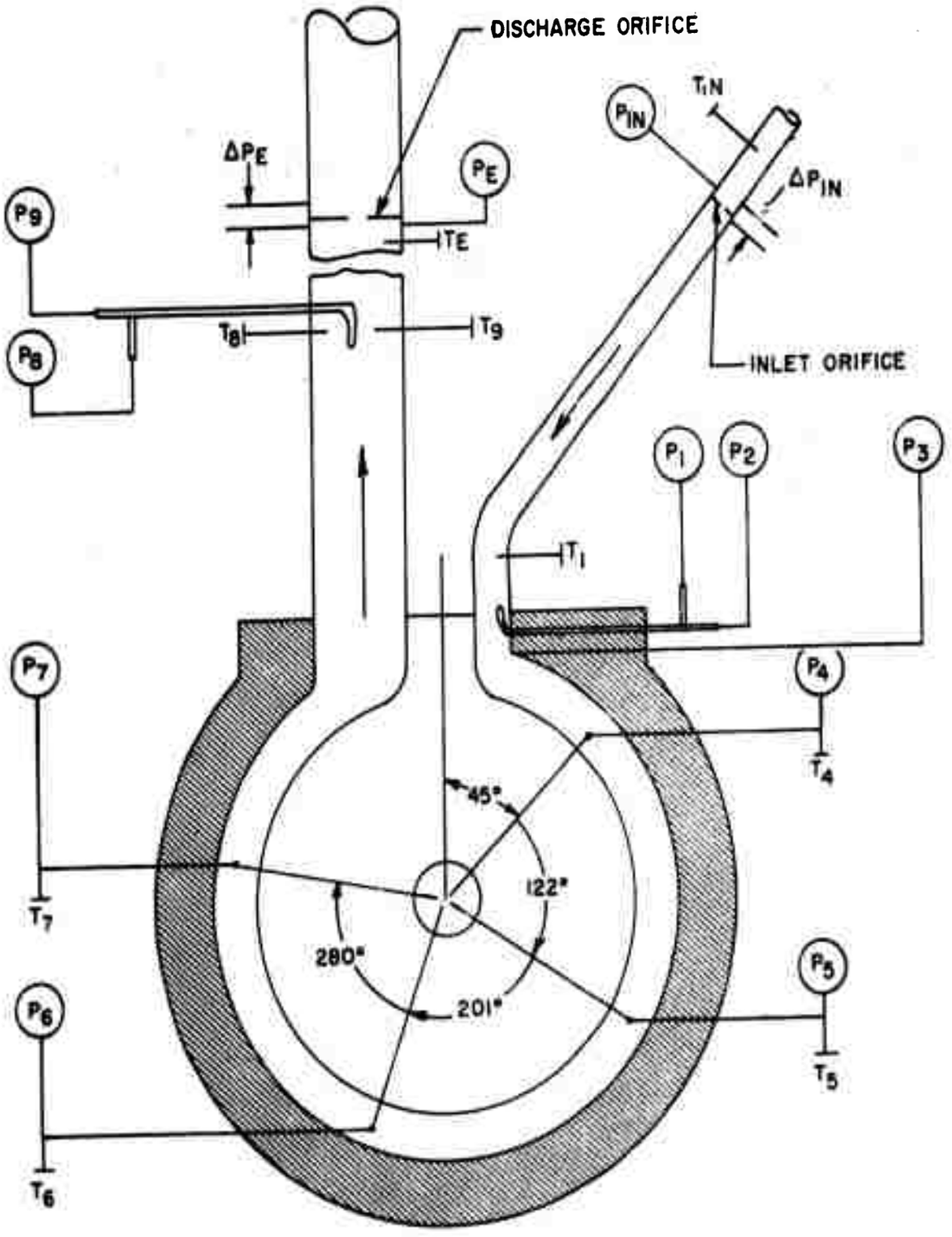

FIGURE 22.

SCHEMATIC-PERIPHERAL DRAG TURBINE INSTRUMENTATION

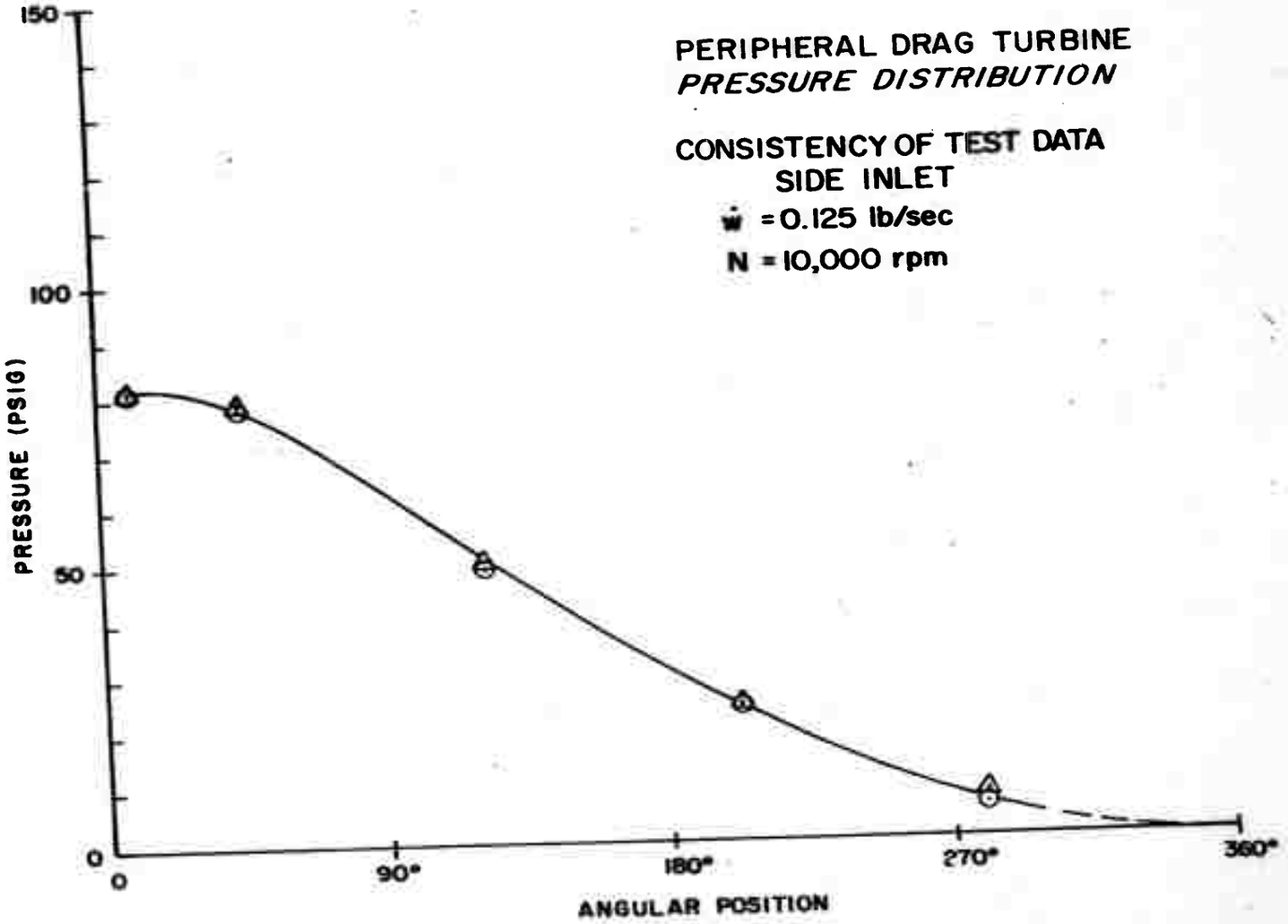

FIGURE 23.

SUNDSTRAND TURBO

DIVISION OF SUNDSTRAND CORPORATION

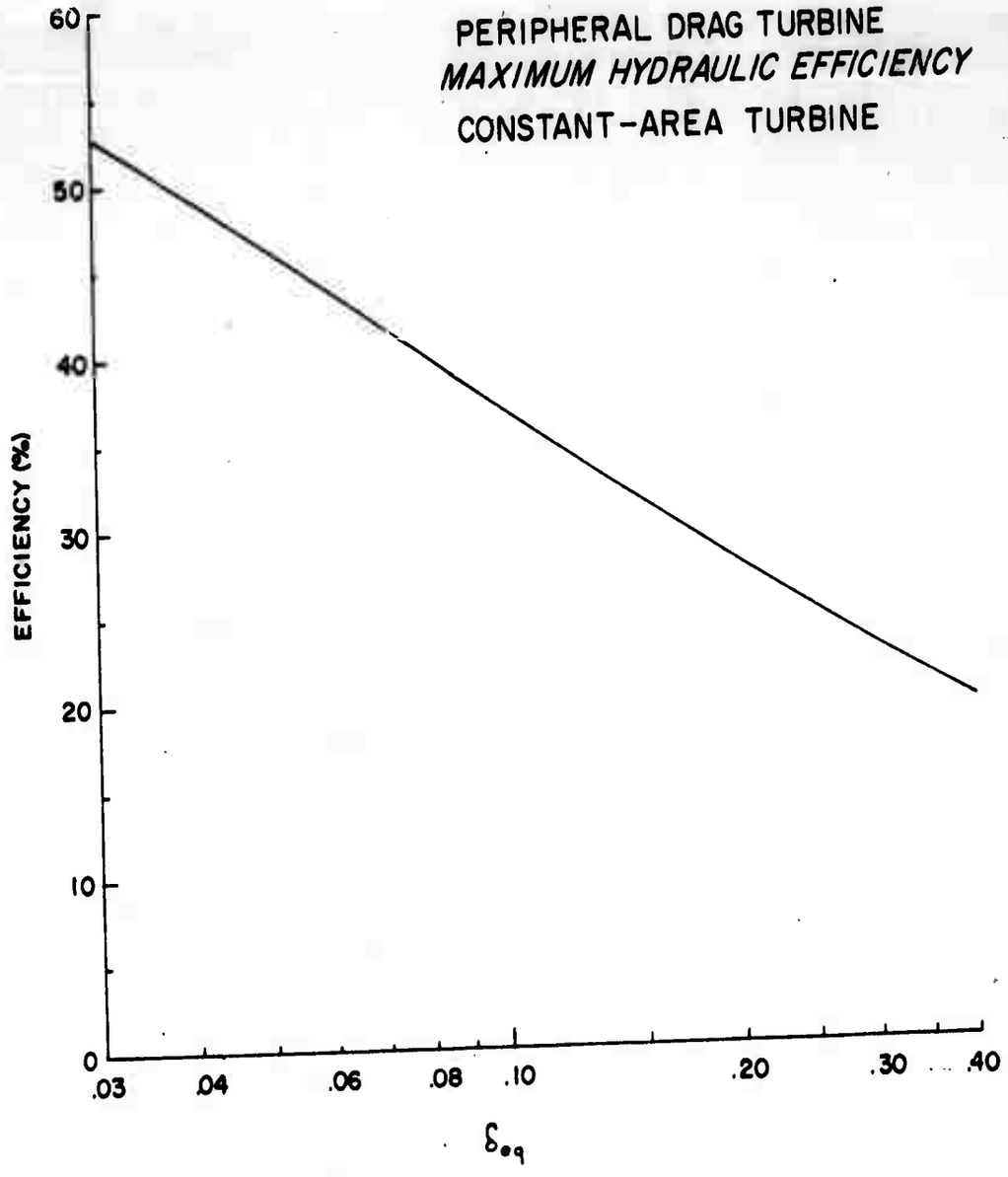
PERIPHERAL DRAG TURBINE
MAXIMUM HYDRAULIC EFFICIENCY
CONSTANT-AREA TURBINE
EFFICIENCY (%)
60
50
40
30
20
10
0
.03
.04
.06
.08
.10
.20
.30
.40
δ_{eq}

FIGURE B-1.

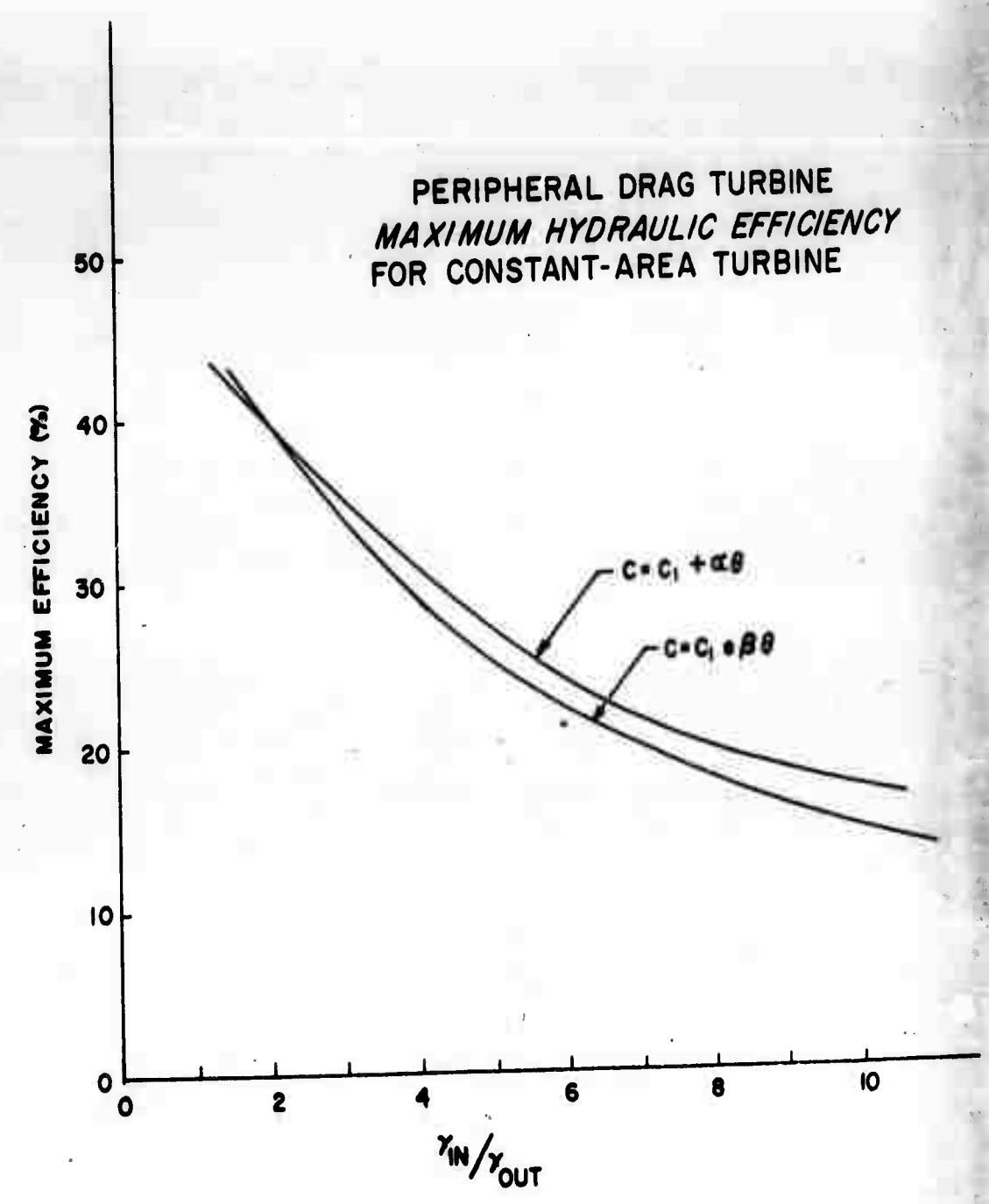
PERIPHERAL DRAG TURBINE
MAXIMUM HYDRAULIC EFFICIENCY
FOR CONSTANT-AREA TURBINE
MAXIMUM EFFICIENCY (%)
50
40
30
20
10
0
0
2
4
6
8
10
γ_{IN}/γ_{OUT}
$C = C_1 + \alpha\beta$
$C = C_1 * \beta\theta$

FIGURE B-2.

UNCLASSIFIED